cantly correlated with WC, SBA, DBP, TG, HDL-C, HbA1c, creatinine, UA, tHCY, and CIMT (Table 2).

By multiple linear regression analysis adjusted for confounding factors, CAVI was significantly correlated with age, SBP, DBP, HbA1c tHCY in all subjects (Table 3). Also, CAVI was significantly correlated with CIMT. On the other hand, CAVI was not significantly correlated with TC, TG, HDL-C, and LDL-C.

Table 3 Multiple Linear Regression Analysis of CAVI With Relevant Factors Adjusted for Confounding Factors

	β	*95%CI*	*p value*
Age	*0.056*	*0.048, 0.063*	*<0.001*
Sex	*0.39*	*0.20, 0.59*	*<0.001*
WC	*–0.005*	*–0.012, 0.003*	*0.24*
SBP	*0.006*	*0.002, 0.009*	*0.002*
TG	*0.17*	*–0.20, 0.54*	*0.36*
HDL-C	*0.003*	*–0.002, 0.008*	*0.21*
HbA1c	*0.18*	*0.062, 0.29*	*0.003*
Creatinine	*–0.27*	*–0.70, 0.15*	*0.21*
UA	*–0.012*	*–0.069, 0.044*	*0.67*
tHCY	*0.4*	*0, 0.80*	*0.05*
CIMT	*0.81*	*0.37, 1.26*	*<0.001*

β, regression coefficient.
CI, confidence interval. Other abbreviations as in Table 1.

Discussion

In this study, we screened CAVI in adults from the Japanese general population and showed that it is independently associated with age, sex, SBP, HbA1c. tHCY and CIMT. Previous research has shown that in vivo aortic stiffness decreases sharply with age in the first decade of life, reaching a minimum at 10 years of age, and thereafter increases with age in both genders[19] The increase in central artery stiffness with age is responsible for earlier wave reflections and changes in pressure wave contours, and cross-sectional studies have shown that aortic PWV (aPWV) increases with age by approximately $0.1\ m \cdot s^{-1} \cdot year^{-1}$[20]. However, we demonstrated that CAVI increases with age about 0.066/year in this study, which suggests that CAVI, as with PWV, can serve as a marker for the increase in central artery stiffness with age.

CAVI is designed not to be affected by BP during measurement, but is probably affected by long-term hypertension. By simple linear regression analysis, Shirai et al recently reported that compared with baPWV, CAVI correlated weakly with SBP and did not correlate with DBP in patients on hemodialysis[12] However, we observed a significant correlation between CAVI and SBP/DBP in both men and women by simple linear regression analysis, and showed that CAVI independently correlated with SBP, after adjustment for confounding factors. In the general population, CAVI may reflect BP, whereas it is essentially independent of changes in BP during examination.

Although there is no doubt that LDL-C directly participates in atherosclerosis and is a major risk factor for CVD, we showed that CAVI was not significantly correlated with HDL-C or LDL-C. Previous reports also indicated a lack of association between baPWV and LDL-C;[21,22] suggesting that further evaluation of LDL-C, in combination with apolipoprotein B, which is a reasonable index of the number of LDL particles, might be appropriate to clarify the effect of lipid metabolism on CAVI.

We are the first to show that CAVI correlates with CIMT, after adjustment for confounding factors, in the general population. Currently, measurement of CIMT is widely used as a noninvasive method of quantifying arterial wall thickening and atherosclerosis progression, and increased CIMT has been shown to be a strong predictor of cardiovascular morbidity and mortality[4,23] Kobayashi et al reported that in patients with risk factors for atherosclerosis, CIMT was independently related to baPWV, and they suggested that the combination of CIMT and baPWV might give reliable information on clinical or subclinical atherosclerosis[10] Furthermore, Okura et al recently showed a significant positive correlation between CAVI and IMT by simple linear regression analysis in patients with hypertension[24] As with baPWV, the measurement of CAVI requires only a few minutes for the entire procedure. Our current results suggest that measurement of CAVI in combination with CIMT might be appropriate for screening of the general population, as well as for patients with atherosclerosis risk factors and for large-scale studies.

Interestingly, we observed that CAVI significantly correlated with HbA1c in the general population after adjustment for confounding factors. It has been reported that baPWV is associated with fasting insulin levels and insulin-related factors, including HbA1c, leading to reduced insulin sensitivity;[25] and our results suggest that, as with baPWV, CAVI may reflect glucose intolerance and possible insulin sensitivity. Further evaluation to clarify the relationship between CAVI and insulin sensitivity is needed.

After adjustment for confounding factors, CAVI was significantly correlated with tHCY, although we did not observe any differences in CAVI between the *CC* and *CT* vs *TT* genotypes of *C667T/MTHFR*. The association between baPWV and HCY is still controversial. Mayer et al evaluated the association between aPWV and tHCY in the general population and found a positive association, even after adjustment for conventional cardiovascular risk factors;[26] On the other hand, de Bree et al conducted a similar cross-sectional analysis and concluded that tHCY concentration was not associated with arterial stiffness;[27] In our study group, CIMT was significantly correlated with tHCY after adjustment for age and sex, which suggests that tHCY might be a marker relevant to atherosclerosis. However, we observed a complete lack of association of CAVI and *C667T/MTHFR* (data not shown), which suggests that careful elaboration is needed for the evaluation of HCY as a screening marker for atherosclerosis.

Study Limitations

First, we could not evaluate the current medication of participants, which might influence the values of CAVI and other markers, nor did we evaluate information about past/present history of coronary risk factors (hypertension, diabetes, hyperlipidemia and smoking). We also could not evaluate the relationship between CAVI and other atherosclerotic markers, such as high-sensitivity C-reactive protein and adipocytokines, including adiponectin and leptin.

Conclusion

We screened CAVI in adults from the Japanese general population, and our results indicate that it may be appropriate as a screening tool for atherosclerosis. Further studies are needed to establish a convenient and effective screening system for atherosclerosis using this technique.

Acknowledgments

This work was financially supported by a Grant-in-Aid from the Japan Society for the Promotion of Science (Nos. 16370106 and 17590546), and by Fukuda Memorial Foundation for Medical Technologies.

References

1. World Health Organization. The Atlas of Heart Disease and Stroke, Website. Avaliable at: http://www.who.int/cardiovascular_diseases/resources/atlas/en/index.html; Accessing website 12 November 2007.
2. Murray CLJ, Lopez AD. Alterative projections of mortality and disability by cause 1990–2020: Global Burden of Disease Study. *Lancet* 1997; **349:** 1498–1504.
3. Vogel RA, Benitez MR. Noninvasive assessment of cardiovascular risk: From Framingham to the future. *Rev Cardiovasc Med* 2000; **1:** 34–42.
4. Bots ML, Hoes AW, Koudstaal PJ, Hofman A, Grobbee DE. Common carotid intima-media thickness and risk of stroke and myocardial infarction: The Rotterdam Study. *Circulation* 1997; **96:** 1432–1437.
5. van Popele NM, Grobbee DE, Bots ML, Asmar R, Topouchian J, Reneman RS, et al. Association between arterial stiffness and atherosclerosis: The Rotterdam Study. *Stroke* 2001; **32:** 454–460.
6. Blacher J, Asmar R, Djane S, London GM, Safar ME. Aortic pulse wave velocity as a marker of cardiovascular risk in hypertensive patients. *Hypertension* 1999; **33:** 1111–1117.
7. Shokawa T, Imazu M, Yamamoto H, Toyofuku M, Tasaki N, Okimoto T, et al. Pulse wave velocity predicts cardiovascular mortality: Findings from the Hawaii-Los Angeles-Hiroshima study. *Circ J* 2005; **69:** 259–264.
8. Yambe T, Yoshizawa M, Saijo Y, Yamaguchi T, Shibata M, Konno S, et al. Brachio-ankle pulse wave velocity and cardio-ankle vascular index (CAVI). *Biomed Pharmacother* 2004; **58:** S95–S98.
9. Imanishi R, Seto S, Toda G, Yoshida M, Ohtsuru A, Koide Y, et al. High brachial-ankle pulse wave velocity is an independent predictor of the presence of coronary artery disease in men. *Hypertens Res* 2004; **27:** 71–78.
10. Kobayashi K, Akishita M, Yu W, Hashimoto M, Ohni M, Toba K. Interrelationship between non-invasive measurement of atherosclerosis: Flow-mediated dilation of brachial artery, carotid intima-media thickness and pulse wave velocity. *Atherosclerosis* 2004; **173:** 13–18.
11. Kubozono T, Miyata M, Ueyama K, Nagaki A, Otsuji Y, Kusano K, et al. Clinical significance and reproducibility of new arterial distensibility index. *Circ J* 2007; **71:** 89–94.
12. Shirai K, Utino J, Otsuka K, Takata M. A novel blood pressure-independent arterial wall stiffness parameter; cardio-ankle vascular index (CAVI). *J Atheroscler Thromb* 2006; **13:** 101–107.
13. Huang CL, Chen MF, Jeng JS, Lin LY, Wang WL, Feng MH, et al. Postchallenge hyperglycaemic spike associated with arterial stiffness. *Int J Clin Pract* 2007; **61:** 397–402.
14. Yambe T, Meng X, Hou X, Wang Q, Sekine K, Shiraishi Y, et al. Cardio-ankle vascular index (CAVI) for the monitoring of the atherosclerosis after heart transplantation. *Biomed Pharmacother* 2005; **59:** S177–S179.
15. Yagura C, Takamura N, Kadota K, Nagazumi T, Morishita Y, Nakazato M, et al. Evaluation of cardiovascular risk factors and related clinical markers in healthy young Japanese adults. *Clin Chem Lab Med* 2007; **45:** 220–225.
16. de Bree A, Verschuren WM, Kromhout D, Kluijtmans LA, Blom HJ. Homocysteine determinants and the evidence to what extent homocysteine determines the risk of coronary heart disease. *Pharmacol Rev* 2002; **54:** 599–618.
17. Garcia AJ, Apitz-Castro R. Plasma total homocysteine quantification: An improvement of the classical high-performance liquid chromatographic method with fluorescence detection of the thiol-SBD derivatives. *J Chromatogr B* 2002; **779:** 359–363.
18. Hara T, Takamura N, Akashi S, Nakazato M, Maeda T, Wada M, et al. Evaluation of clinical markers of atherosclerosis in young and elderly Japanese adults. *Clin Chem Lab Med* 2006; **44:** 824–829.
19. Benetos A, Waeber B, Izzo J, Mitchell G, Resnick L, Asmar R, et al. Influence of age, risk factors, and cardiovascular and renal disease on arterial stiffness: Clinical applications. *Am J Hypertens* 2002; **15:** 1101–1108.
20. Asmar R, Benetos A, London G, Hugue C, Weiss Y, Topouchian J, et al. Aortic distensibility in normotensive, untreated and treated hypertensive patients. *Blood Press* 1995; **4:** 48–54.
21. Hansen TW, Jeppesen J, Rasmussen S, Ibsen H, Torp-Pedersen C. Relation between insulin and aortic stiffness: A population-based study. *J Hum Hypertens* 2004; **18:** 1–7.
22. Okamura T, Moriyama Y, Kadowaki T, Kanda H, Ueshima H. Non-invasive measurement of brachial-ankle pulse wave velocity is associated with serum C-reactive protein but not with alpha-tocopherol in Japanese middle-aged male workers. *Hypertens Res* 2004; **27:** 173–180.
23. Chambless LE, Folsom AR, Clegg LX, Sharrett AR, Shahar E, Nieto FJ, et al. Carotid wall thickness is predictive of incident clinical stroke: The *Atherosclerosis* Risk in Communities (ARIC) study. *Am J Epidemiol* 2000; **151:** 478–487.
24. Okura T, Watanabe S, Kurata M, Manabe S, Koresawa M, Irita J, et al. Relationship between Cardio-Ankle Vascular Index (CAVI) and carotid atherosclerosis in patients with essential hypertension. *Hypertens Res* 2007; **30:** 335–340.
25. Tsubakimoto A, Saito I, Mannami T, Naito Y, Nakamura S, Dohi Y, et al. Impact of metabolic syndrome on brachial-ankle pulse wave velocity in Japanese. *Hypertens Res* 2006; **29:** 29–37.
26. Mayer O, Filipovsky J, Dolejsova M, Cifkova R, Simon J, Bolek L. Mild hyperhomocysteinaemia is associated with increased aortic stiffness in general population. *J Hum Hypertens* 2006; **20:** 267–271.
27. de Bree A, Mennen LI, Zureik M, Ducros V, Guilland JC, Nicolas JP, et al. Homocysteine is not associated with arterial thickness and stiffness in healthy middle-aged French volunteers. *Int J Cardiol* 2006; **113:** 332–340.

Immunity
Article

Indispensable Role of the Runx1-Cbfβ Transcription Complex for In Vivo-Suppressive Function of FoxP3$^+$ Regulatory T Cells

Akihiko Kitoh,[1,2] Masahiro Ono,[1,2,3] Yoshinori Naoe,[4] Naganari Ohkura,[1,3,5] Tomoyuki Yamaguchi,[1] Hiroko Yaguchi,[1,3,5] Issay Kitabayashi,[6] Toshihiko Tsukada,[5] Takashi Nomura,[1] Yoshiki Miyachi,[2] Ichiro Taniuchi,[4] and Shimon Sakaguchi[1,3,*]
[1]Department of Experimental Pathology, Institute for Frontier Medical Sciences
[2]Department of Dermatology
Graduate School of Medicine, Kyoto University, Kyoto 606-8507, Japan
[3]Laboratory of Experimental Immunology, WPI Immunology Frontier Research Center, Osaka University, Suita 565-0871, Japan
[4]Laboratory for Transcriptional Regulation, RIKEN Research Center for Allergy and Immunology, Kanagawa 230-0045, Japan
[5]Tumor Endocrinology Project
[6]Molecular Oncology Division
National Cancer Center Research Institute, Tokyo 104-0045, Japan
*Correspondence: shimon@frontier.kyoto-u.ac.jp
DOI 10.1016/j.immuni.2009.09.003

SUMMARY

Naturally arising regulatory T (Treg) cells express the transcription factor FoxP3, which critically controls the development and function of Treg cells. FoxP3 interacts with another transcription factor Runx1 (also known as AML1). Here, we showed that Treg cell-specific deficiency of Cbfβ, a cofactor for all Runx proteins, or that of Runx1, but not Runx3, induced lymphoproliferation, autoimmune disease, and hyperproduction of IgE. *Cbfb*-deleted Treg cells exhibited impaired suppressive function in vitro and in vivo, with altered gene expression profiles including attenuated expression of FoxP3 and high expression of interleukin-4. The Runx complex bound to more than 3000 gene loci in Treg cells, including the *Foxp3* regulatory regions and the *Il4* silencer. In addition, knockdown of *RUNX1* showed that RUNX1 is required for the optimal regulation of FoxP3 expression in human T cells. Taken together, our results indicate that the Runx1-Cbfβ heterodimer is indispensable for in vivo Treg cell function, in particular, suppressive activity and optimal expression of FoxP3.

INTRODUCTION

CD4$^+$CD25$^+$FoxP3$^+$ naturally occurring regulatory T (Treg) cells play essential roles for the maintenance of immunological self-tolerance and immune homeostasis by actively suppressing aberrant or excessive immune responses harmful to the host (Sakaguchi et al., 2006). Natural Treg cells specifically express the transcription factor FoxP3, which critically controls the development and the function of Treg cells as illustrated by *FOXP3* mutations (Ochs et al., 2005). FoxP3 deficiency or dysfunction in humans results in the development of IPEX (immune dysregulation, polyendocrinopathy, enteropathy, X-linked) syndrome, which is characterized by severe autoimmune disease, allergy, and inflammatory bowel disease (Sakaguchi et al., 2006). FoxP3 expression can confer suppressive activity to Treg cells, suppress the production of cytokines such as interleukin-2 (IL-2) and interferon-gamma (IFN-γ), and upregulate the expression of Treg cell-associated molecules including CD25 and cytotoxic T lymphocyte-associated antigen 4 (CTLA-4) (Fontenot et al., 2003; Hori et al., 2003; Khattri et al., 2003). Recent studies have shown that the gene regulatory function of FoxP3 requires its association with other transcription factors, such as NFAT (nuclear factor of activated T cells), NF-κB (nuclear factor-κB), and Runx1 (runt-related transcription factor 1), also known as AML1 (acute myeloid leukemia 1), and with histone deacetylases and acetyltransferases (Bettelli et al., 2005; Li et al., 2007; Ono et al., 2007; Wu et al., 2006). Yet, the precise molecular mechanisms by which FoxP3 controls Treg cell function remain to be elucidated.

The Runx (AML) transcription factors consist of three members: Runx1 (AML1), Runx2 (AML3), and Runx3 (AML2) (van Wijnen et al., 2004). All Runx proteins bind to the specific DNA consensus sequences (ACCACA) via a highly conserved DNA-binding *runt* domain. Runx binding is stabilized by the association with Cbfβ (core-binding factor β), a non-DNA-binding cofactor essential for the function of all Runx proteins (Speck, 2001). The Runx-Cbfβ heterodimeric complex interacts with other DNA-binding transcription factors, coactivators, or corepressors to either activate or repress expression of the target genes in a context-dependent manner (Durst and Hiebert, 2004; Taniuchi and Littman, 2004). In addition to the essential requirement of Runx proteins for definitive hematopoiesis (de Bruijn and Speck, 2004), Runx1 and Runx3 are crucially involved in the differentiation and function of peripheral T cells (Djuretic et al., 2007; Komine et al., 2003; Naoe et al., 2007; Zhang et al., 2008) as well as thymic T cell development (Grueter et al., 2005; Sato et al., 2005; Setoguchi et al., 2008; Taniuchi et al., 2002; Woolf et al., 2003). We have previously shown that Runx1 binds to the promoter of the *Il2* and *Ifng* genes and upregulates the production of IL-2 and IFN-γ, respectively. Further, FoxP3 binds to Runx1 in Treg cells, thereby repressing *Il2* and *Ifng* and

activating the genes encoding CD25 (*Il2ra*) and CTLA-4 (*Ctla4*) (Ono et al., 2007). We have also shown that, in vitro, FoxP3 can interact with the other members of the Runx family, Runx2 and Runx3, in addition to Runx1 (Ono et al., 2007). These findings collectively suggest that the Runx-dependent transcription program operating in conventional T cells could be modulated in Treg cells through interaction with FoxP3. Yet, it remains obscure whether the Runx-mediated gene regulation is indeed required for the in vivo function of Treg cells.

In this report, we have generated mice with Treg cell-specific conditional deletion of *Cbfb* to analyze in vivo the possible contribution of Runx-dependent gene regulation to Treg cell function because all Runx proteins need to form a heterodimeric complex with Cbfβ for exerting transcriptinal activities and Cbfβ deficiency disrupts the function of the Runx complex (Speck, 2001). Here, we showed that Treg cell-specific Cbfβ-deficient mice spontaneously developed lymphoproliferation, autoimmune disease, and IgE hyperproduction and that *Cbfb*-deleted Treg cells exhibited impaired suppressive activity both in vitro and in vivo. In addition, Treg cell-specific conditional deletion of *Runx1*, but not *Runx3*, led to the development of immunological diseases similar to those observed in Treg cell-specific Cbfβ deficiency. Our findings thus indicate that the heterodimeric Runx1-Cbfβ complex is an indispensable transcription regulator for in vivo functions of Treg cells and that it is a potential therapeutic target for controlling physiological and pathological immune responses.

RESULTS

Treg Cell-Specific Deletion of *Cbfb* and the Resulting Development of Autoimmune Disease

To determine whether Runx proteins were required for in vivo function of FoxP3$^+$ Treg cells, we generated Treg cell-specific *Cbfb*-deleted mice by crossing mice harboring *LoxP*-flanked *Cbfb* allele with *Foxp3-Ires-Cre* (*FIC*) knockin mice, which faithfully express Cre recombinase in FoxP3$^+$ T cells (Naoe et al., 2007; Wing et al., 2008). FIC-mediated genomic deletion of *LoxP*-flanked region occurred in almost 100% CD4$^+$FoxP3$^+$ cells and a small population of CD8$^+$ T cells (Wing et al., 2008). With genomic DNA-PCR analyses of subpopulations of thymocytes and splenic T cells from *Cbfb$^{F/F}$: FIC* mice, inactivation of the *Cbfb* gene was initiated specifically in CD4-single positive (CD4SP) HSA^{lo}CD25^{hi} mature thymocytes and was completed in CD4$^+$CD25^{hi} splenic T cells, indicating Treg cell-specific deletion of the *Cbfb* gene (Figure 1A, left). Some of the CD4$^+$CD25$^-$ T cells also harbored the genomic *Cbfb* deletion (Figure 1A, left). This can be attributed to the presence of CD4$^+$CD25$^-$FoxP3$^+$ Treg cells in this CD4$^+$CD25$^-$ population (Figure S1 and Supplemental Data available online). As a consequence of the gene inactivation, the Cbfβ protein was undetectable in CD4$^+$CD25^{hi} splenocytes, although a substantial amount of the Cbfβ protein remained in CD4SP HSA^{lo}CD25^{hi} thymocytes (Figure 1A, right). Thus, the Cbfβ protein is gradually decreased in FoxP3$^+$ cells after *Cbfb* gene deletion in the thymus and almost completely lost in the periphery, which is consistent with a similar finding with conditional *Cbfb* deletion by *Cd4-Cre* transgene (Naoe et al., 2007).

Notably, *Cbfb$^{F/F}$: FIC* mice spontaneously developed severe lymphadenopathy and splenomegaly with significantly increased numbers of splenocytes by 14 weeks of age (Figure 1B). Various types of immune cells including CD4$^+$ T cells, CD8$^+$ T cells, B cells, macrophages, and dendritic cells increased in the enlarged spleens of *Cbfb$^{F/F}$: FIC* mice (Figure S2). Seventy percent of *Cbfb$^{F/F}$: FIC* mice developed histologically evident gastritis accompanying high titers of anti-gastric parietal cell autoantibodies in the sera, whereas control *Cbfb$^{F/+}$: FIC* littermates did not (Figures 1C and 1D). Flow cytometric analysis revealed that non-Treg T cells, i.e., CD4$^+$FoxP3$^-$ conventional T cells and CD8$^+$ T cells, in *Cbfb$^{F/F}$: FIC* mice showed an activated or memory phenotype; e.g., CD69$^+$, CD122$^+$, CD44^{hi}, and CD62L^{lo} (Figure 1E). CD4$^+$ and CD8$^+$ T cells abundantly produced cytokines such as IFN-γ, IL-2, IL-4, and IL-10, as revealed by intracellular cytokine staining after stimulation with PMA and ionomycin (Figure 1F). In addition, *Cbfb$^{F/F}$: FIC* mice showed 10-fold elevated concentrations of serum IgE and 1.5-fold increase in serum IgG (Figure 1G). Thus, Treg cell-specific Cbfβ deficiency produced autoimmune disease and led to hyperproduction of IgE.

The Effects of Treg Cell-Specific *Cbfb* Gene Deletion on Treg Cell Development and Function

To analyze the mechanism of autoimmunity caused by Treg cell-specific *Cbfb* deficiency, we attempted to determine whether thymic generation and differentiation of Treg cells, their peripheral survival, or their suppressive function was affected by the deficiency.

There was no significant difference in the number of total or FoxP3$^+$ thymocytes between *Cbfb$^{F/F}$: FIC* and *Cbfb$^{F/+}$: FIC* mice (Figure 2A and Figure S3). HSA^{lo}CD25^{hi}FoxP3$^+$CD4SP thymic Treg cells normally developed in *Cbfb$^{F/F}$: FIC* mice as in control *Cbfb$^{F/+}$: FIC* mice (Figure 2B). Whereas Runx proteins were required for the differentiation of immature thymocytes to TCRβ^{hi}HSA^{lo}CD4SP mature thymocytes (Egawa et al., 2007), the generation of FoxP3$^+$TCRβ^{hi}HSA^{lo}CD4SP mature thymocytes was not markedly impaired in *Cbfb$^{F/F}$: FIC* mice (Figure S4). Residual Cbfβ protein might be sufficient to support differentiation and maturation of FoxP3$^+$ cells in the thymus (Figure 1A).

We next examined whether Treg cell homeostasis was impaired in the periphery of *Cbfb*-deleted mice. The proportion of CD4$^+$FoxP3$^+$ Treg cells to total CD4$^+$ T cells and the absolute number of Treg cells were slightly higher in *Cbfb$^{F/F}$: FIC* mice than in *Cbfb$^{F/+}$: FIC* mice (Figures 2C and 2D). Notably, Treg cells in *Cbfb$^{F/F}$: FIC* mice showed substantially decreased expression of FoxP3, compared to those in control mice (Figure 2D). Expression of Ki-67, a cellular marker for proliferation, indicated that an equivalent or larger proportion of Treg cells were active in cell cycle in *Cbfb$^{F/F}$: FIC* mice compared with control mice (Figure 2E). In *Cbfb$^{F/F}$: FIC* mice, Ki-67$^-$ resting Treg cells showed reduced expression of FoxP3, whereas Ki-67^{hi} proliferating Treg cells expressed FoxP3 at equivalent amounts as Ki-67^{hi} Treg cells in control mice (Figure 2E). In vivo BrdU labeling also revealed that CD4$^+$CD25^{hi} splenocytes in *Cbfb$^{F/F}$: FIC* mice were more actively proliferating than those in *Cbfb$^{F/+}$: FIC* mice (Figure 2F). Treg cells in the former expressed only slightly lower amounts of CD127 (IL-7 receptor α chain) and were not apoptotic according to 7-AAD (7-amino-actinomycin D) and Annexin V staining, in accord with the previous finding that *Runx1*-deficient

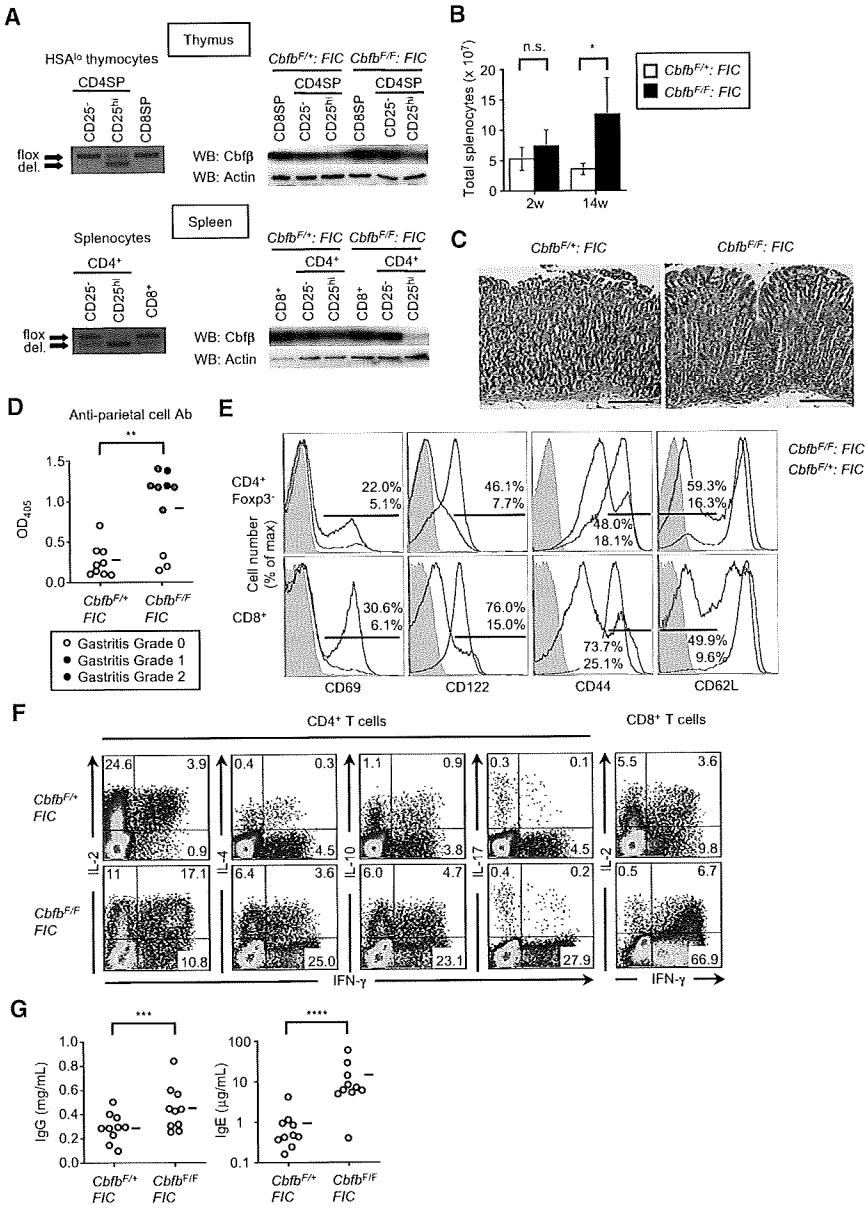

Figure 1. Treg Cell-Specific *Cbfb* Deficiency Induced Autoimmune Disease and Hyperproduction of IgE

(A) Treg cell-specific *Cbfb* deletion in *Cbfb*$^{F/F}$: *FIC* mice. PCR analysis (left) for detecting *Cbfb*^{F} (flox) and *Cbfb*-deleted (del.) alleles of the *Cbfb* gene was performed with genomic DNA from indicated thymocyte (top) and splenocyte (bottom) subpopulations of *Cbfb*$^{F/F}$: *FIC* mice as templates. Immunoblot analysis (right) of Cbfβ protein expression in indicated thymocyte (top) and splenocyte (bottom) subpopulations of *Cbfb*$^{F/F}$: *FIC* and control *Cbfb*$^{F/+}$: *FIC* littermates is shown. Results representative of two experiments are shown.

(B) The absolute numbers of total splenocytes are shown as the mean ± SD value from *Cbfb*$^{F/F}$: *FIC* mice and *Cbfb*$^{F/+}$: *FIC* littermates (n = 4) at 2 and 14 weeks of age. *p = 0.02.

(C) Hematoxylin and eosin staining of sections from stomachs of 7- to 8-week-old *Cbfb*$^{F/F}$: *FIC* and *Cbfb*$^{F/+}$: *FIC* littermates (n = 10). Representative photomicrographs are shown. Scale bars represent 10.0 μm.

(D) Titers of parietal cell autoantibodies in the sera of 8-week-old *Cbfb*$^{F/F}$: *FIC* and *Cbfβ*$^{F/+}$: *FIC* littermates (n = 10) were assessed by ELISA. Horizontal lines represent averages from each group. **p = 0.01.

(E) Activated surface-marker phenotype of CD4^{+}FoxP3^{-} conventional T cells and CD8^{+} T cells in *Cbfb*$^{F/F}$: *FIC* mice at 16 weeks of age. Data are representative of five experiments.

(F) Production of proinflammatory cytokines by CD4^{+} and CD8^{+} T cells in *Cbfb*$^{F/F}$: *FIC* mice at 14 weeks of age. Data are representative of three experiments.

(G) Titers of IgG and IgE in the sera of 8-week-old *Cbfb*$^{F/F}$: *FIC* and *Cbfb*$^{F/+}$: *FIC* littermates (n = 10) were assessed by ELISA. Horizontal lines represent averages from each group. ***p = 0.04; ****p = 0.001.

Treg cells in *Runx1*$^{F/F}$: *Cd4-Cre* mice were apoptosis resistant (Egawa et al., 2007) (Figures 2G and 2H).

Phenotypically, *Cbfb*-deleted Treg cells expressed CD25 and glucocorticoid-induced tumor necrosis factor receptor family-related protein (GITR) at higher amounts and CTLA-4 at equivalent amounts compared to control Treg cells, whereas they scarcely expressed CD103 in accord with the finding that Runx3 controls CD103 expression (Grueter et al., 2005) (Figure 3A). Neither *Cbfb*-deleted nor control Treg cells proliferated in response to in vitro polyclonal TCR stimulation with anti-CD3 (Figure 3B). Yet, *Cbfb*-deleted Treg cells were less suppressive in vitro (Figure 3C). In addition, they failed to prevent the development of colitis and weight loss in SCID mice when cotransferred with BALB/c CD4^{+}CD25^{-}CD45RB^{hi} T cells, in contrast to effective disease prevention by cotransfer of control Treg cells (Figures 3D–3F). Similarly, *Cbfb*-deleted Treg cells failed to suppress the development of gastritis (data not shown). *Cbfb*-deleted Treg cells survived when transferred to SCID mice (Figure S5A), indicating that the impaired in vivo suppressive activity of *Cbfb*-deleted Treg cells was not due to their shorter survival. In addition, the attenuated CD103 expression in *Cbfb*-deleted Treg cells (Figure S5B) would not be responsible for the impaired Treg cell function because others reported that Treg cell-mediated control of colitis did not require CD103 expression by Treg cells (Annacker et al., 2005).

Collectively, these findings indicate that failure in Treg cell-mediated self-tolerance in *Cbfb*$^{F/F}$: *FIC* mice is not due to numerical deficiency, reduced proliferation, or enhanced apoptosis of FoxP3^{+} Treg cells, but due to their impaired suppressive activity.

Cbfb-Deleted Treg Cells Show Hyperproduction of IL-4

Treg cells hardly produce cytokines such as IL-2, IFN-γ, and IL-4 (Sakaguchi et al., 2006). Flow cytometric analysis revealed that a larger proportion of FoxP3^{+} Treg cells from *Cbfb*$^{F/F}$: *FIC* mice produced IL-4 and IL-10 compared to Treg cells from control

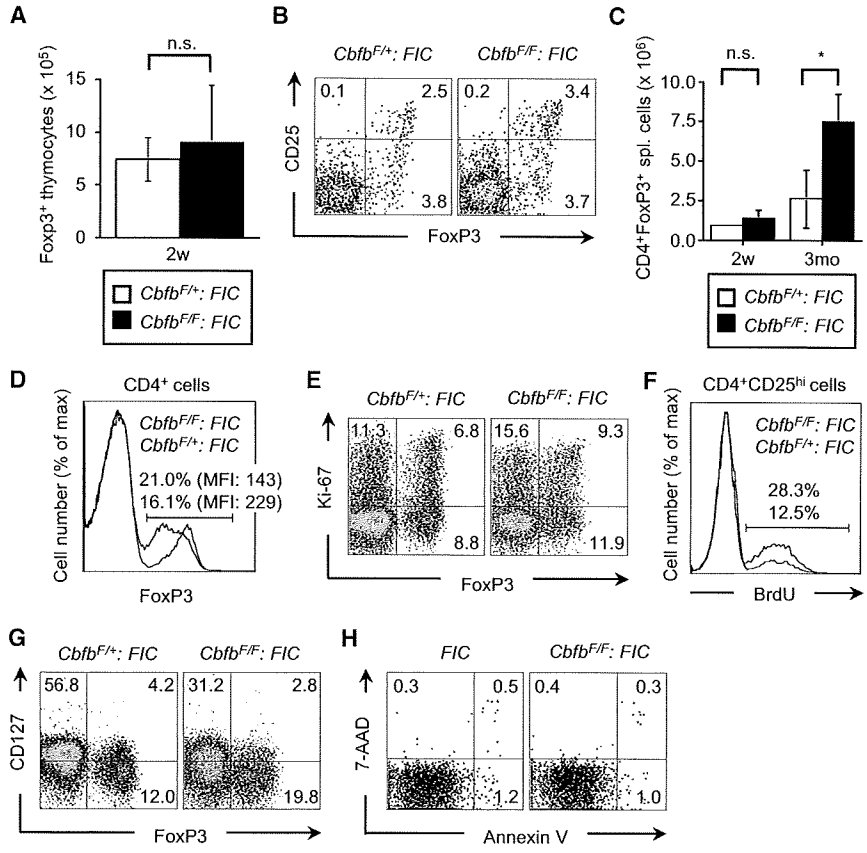

Figure 2. Generation and Homeostasis of Treg Cells in *Cbfb*$^{F/F}$: *FIC* Mice

(A) The absolute numbers of FoxP3$^+$ thymocytes from 2-week-old *Cbfb*$^{F/F}$: *FIC* and *Cbfb*$^{F/+}$: *FIC* littermates (n = 3) are shown as the mean ± SD value.

(B) Expression of CD25 and FoxP3 by CD4SP HSA^{lo} thymocytes from 3-week-old *Cbfb*$^{F/F}$: *FIC* and *Cbfb*$^{F/+}$: *FIC* littermates. Results representative of three experiments are shown.

(C) The absolute numbers of CD4$^+$FoxP3$^+$ splenocytes from *Cbfb*$^{F/F}$: *FIC* and *Cbfb*$^{F/+}$: *FIC* littermates (n = 3) at 2 weeks and 3 months of age are shown as the mean ± SD value. *p = 0.05.

(D) Expression of FoxP3 by CD4$^+$ splenocytes from 7-week-old *Cbfb*$^{F/F}$: *FIC* and *Cbfb*$^{F/+}$: *FIC* littermates. Results representative of five experiments are shown.

(E) Expression of Ki-67 and FoxP3 by CD4$^+$ T cells from 7-week-old *Cbfb*$^{F/F}$: *FIC* and *Cbfb*$^{F/+}$: *FIC* littermates. Data are representative of three experiments.

(F) 9-week-old *Cbfb*$^{F/F}$: *FIC* and *Cbfb*$^{F/+}$: *FIC* littermates were injected with BrdU for 3 days, and incorporation of BrdU into CD4$^+$CD25^{hi} splenocytes was assessed by flow cytometry. Results representative of four experiments are shown.

(G) Expression of CD127 and FoxP3 by CD4$^+$ T cells from 7-week-old *Cbfb*$^{F/F}$: *FIC* and *Cbfb*$^{F/+}$: *FIC* littermates. Results representative of four experiments are shown.

(H) 7-AAD and AnnexinV staining of CD4$^+$CD25^{hi} cells from 8-week-old *Cbfb*$^{F/F}$: *FIC* and littermate control mice. Results representative of two experiments are shown.

mice, whereas there were no substantial differences in the percentage of IL-2- or IFN-γ-producing cells among FoxP3$^+$ Treg cells (Figure 3G). Few IL-17-expressing FoxP3$^+$ Treg cells were present in both groups of mice (Figure 3G). The amount of mRNA for each cytokine in CD4$^+$CD25^{hi} cells in *Cbfb*$^{F/F}$: *FIC* and control mice correlated with the protein expression. However, mRNA for IL-17, which was detectable in *Cbfb*$^{F/+}$: *FIC* mice, was substantially lower in *Cbfb*$^{F/F}$: *FIC* mice (Figure 3H).

Next, the expression of transcription factors *Foxp3*, *Tbx21*, *Gata3*, and *Rorgt*, all of which are essential for Th or Treg cell lineage differentiation, were examined in *Cbfb*-deleted Treg cells. *Foxp3* mRNA expression decreased in *Cbfb*-deleted Treg cells, which is consistent with decreased FoxP3 expression at the protein level (Figure S6). In contrast to the hyperproduction of Th2 cell cytokines IL-4 and IL-10, mRNA expression of Th2 cell-specific transcription factor *Gata3* in *Cbfb*-deleted Treg cells was equivalent to that in control Treg cells, whereas *Cbfb*-deleted Treg cells showed higher expression of Th1 cell-specific transcription factor *Tbx21*. Thus, hyperproduction of Th2 cell cytokines by *Cbfb*-deleted Treg cells was not due to overexpression of *Gata3*, although it has been reported that Runx1 represses *Gata3* expression in conventional CD4$^+$ T cells (Komine et al., 2003). The expression of *Rorgt*, which controls the differentiation of IL-17-producing Th17 cells, also decreased in *Cbfb*-deleted Treg cells compared with control Treg cells (Figure S6). Taken together, our findings show that Cbfβ-deficient Treg cells transcribed *Il17a* and *Rorgt* to lesser extents than control Treg cells, whereas *Il4*, *Il10*, and *Tbx21* were more actively transcribed in the former.

Genes Possibly Associated with Impaired Suppressive Function of *Cbfb*-Deleted Treg Cells

To elucidate the molecular mechanisms underlying the dysfunction of *Cbfb*-deleted Treg cells, we examined gene expression profiles of CD4$^+$CD25^{hi} cells from *Cbfb*$^{F/F}$: *FIC* and littermate *Cbfb*$^{F/+}$: *FIC* mice by expression microarray. We first focused on the previously described "Treg cell signature" genes, which are differentially expressed between Treg cells and conventional CD4$^+$ T cells and therefore thought to be closely related to Treg cell-intrinsic properties including suppressive function (Hill et al., 2007). Sixty-nine signature genes including *Socs2* and *Nrp1* were found to be differentially expressed in *Cbfb*-deleted Treg cells (unpaired t test, $p < 0.05$. see Table S1). Yet, there were not significant differences in the expression of many well-known Treg cell-associated genes, such as *Ctla4*, *Tnfrsf18* (*Gitr*), *Gzmb*, *Folr4*, and *Gpr83*, between *Cbfb*-deleted and control Treg cells (Figure 4A). Decreased mRNA expression of *Itgae* (*CD103*) in *Cbfb*-deleted Treg cells was consistent with the aforementioned flow cytometry results (Figure 4A and Figure 3A). Using the false discovery rate (FDR)-controlling procedure (FDR < 0.2), we further attempted to determine other genes that were differentially expressed in *Cbfb*-deleted Treg cells. We found that 22 and 24 genes were significantly up- or

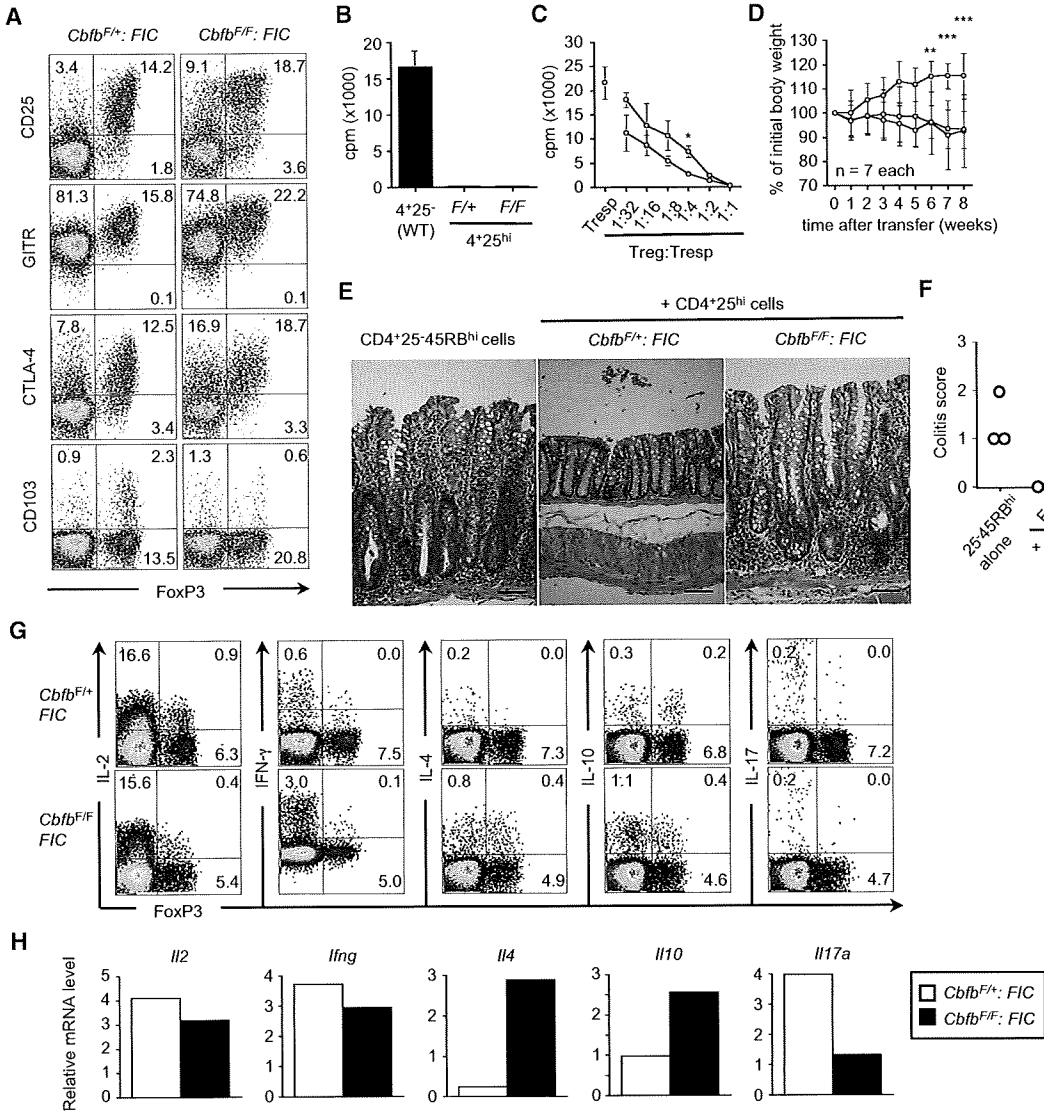

Figure 3. Impaired In Vivo- and In Vitro-Suppressive Activity of *Cbfb*-Deleted Treg Cells

(A) Expression of FoxP3 and other Treg cell-associated molecules by $CD4^+$ T cells from 7-week-old *Cbfb*$^{F/F}$: *FIC* and *Cbfb*$^{F/+}$: *FIC* littermates. Results representative of at least three experiments are shown.

(B) $CD4^+CD25^-$ conventional T cells from wild-type BALB/c mice and $CD4^+CD25^{hi}$ cells from *Cbfb*$^{F/F}$: *FIC* and *Cbfb*$^{F/+}$: *FIC* littermates were stimulated in vitro for 3 days, and cell proliferation was assessed by thymidine incorporation. Data are mean ± SD of triplicates done in one experiment representative of seven.

(C) In vitro suppression assay with $CD4^+CD25^-$ T cells from 6-week-old wild-type BALB/c mice as responders and $CD4^+CD25^{hi}$ T cells from 5-week-old *Cbfb*$^{F/F}$: *FIC* (red lines) or *Cbfb*$^{F/+}$: *FIC* (blue lines) littermates as suppressors. Data are mean ± SD of triplicates done in one experiment representative of four. *p = 0.004 (unpaired t test).

(D) Eight-week-old C.B-17 SCID mice received 4×10^5 $CD4^+CD25^-CD45RB^{hi}$ cells purified from wild-type BALB/c mice either alone (black lines) or together with 3×10^5 $CD4^+CD25^{hi}$ cells purified from 6-week-old *Cbfb*$^{F/F}$: *FIC* (red lines) or *Cbfb*$^{F/+}$: *FIC* (blue lines) littermates. Body weight is represented as the percentage of initial weight (mean ± SD). Results from a total of four independent experiments are shown. **p = 0.01; ***p = 0.02, *Cbfb*$^{F/F}$: *FIC* versus *Cbfb*$^{F/+}$: *FIC* by Mann-Whitney U test.

(E) Hematoxylin and eosin staining of sections from colons of SCID mice transferred as described in (D) (n = 3 each group). Representative photomicrographs are shown. Scale bars represent 10.0 μm.

(F) Colitis were histologically scored (n = 3 each group).

(G) Costaining of FoxP3 and the indicated cytokines in $CD4^+$ T cells from 14-week-old *Cbfb*$^{F/F}$: *FIC* and *Cbfb*$^{F/+}$: *FIC* littermates fter the stimulation with PMA and ionomycin for 6 hr. Results representative of three experiments are shown.

(H) Relative mRNA expression of the indicated cytokines in $CD4^+CD25^{hi}$ cells purified from *Cbfb*$^{F/F}$: *FIC* and *Cbfb*$^{F/+}$: *FIC* littermates at 6 weeks of age. Data are representative of two experiments.

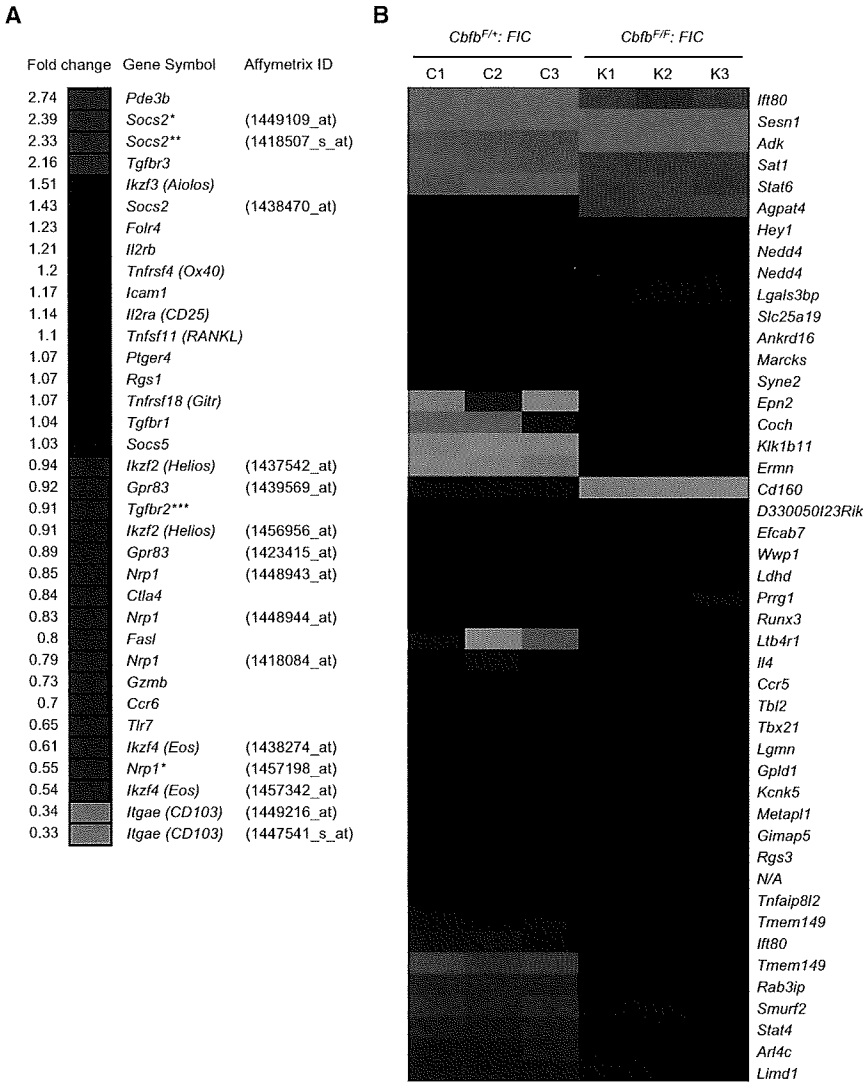

Figure 4. Gene Expression Analysis of Treg Cells in *Cbfb*$^{F/F}$: *FIC* Mice

mRNA expression profiles of CD4$^+$CD25^{hi} T cells from *Cbfb*$^{F/F}$: *FIC* and *Cbfb*$^{F/+}$: *FIC* littermates were analyzed by expression microarray (n = 3). (A) shows fold change in expression of representative "Treg cell signature" genes in CD4$^+$CD25^{hi} T cells from *Cbfb*$^{F/F}$: *FIC* mice versus *Cbfb*$^{F/+}$: *FIC* littermates. *, p = 0.01; **, p = 0.03; ***, p = 0.02 (unpaired t test). (B) shows a heat map of genes differentially expressed in CD4$^+$CD25^{hi} T cells of *Cbfb*$^{F/F}$: *FIC* mice with statistical significance (FDR < 0.2).

downregulated, respectively, in *Cbfb*-deleted Treg cells (Figure 4B and Table S2). Differentially expressed molecules included IL-4, CCR5, leukotriene B4 receptor 1 (Ltb4r1, also called BLT1), and CD160, which are secreted or have extracellular regions possibly involved in cellular interactions.

The Runx Complex Binds to the Regulatory Regions of Many Genes Including *Foxp3* and *Il4*

To further investigate Runx-dependent gene regulation in Treg cells, we attempted to identify target genes of the Runx complex. Genome-wide analysis with chromatin immunoprecipitation (ChIP) coupled with promoter tiling array showed that the Runx complex bound to the promoter regions of 3566 genes including *Foxp3* (Figure 5A and Table S3). Similar analysis with the customized array covering the *Foxp3* gene locus revealed that the Runx complex bound to several regions of the *Foxp3* gene in Treg cells prepared from wild-type BALB/c mice (Figure 5B, left). It has been reported that the following three conserved noncoding sequences (CNSs) contribute to *Foxp3* expression: one CNS located in 0.5 kb upstream of the transcription start site (CNS1) and two CNSs located in the first intron (CNS2 and CNS3) (Kim and Leonard, 2007; Mantel et al., 2006; Tone et al., 2008). The binding of the Runx complex to CNS1 and CNS3 of the *Foxp3* gene in Treg cells was detected, although the binding to CNS2 was not examined because of unavailability of appropriate probes for this region (Figure 5B, left). Conventional ChIP assays revealed that the Runx complex bound to CNS2 as well as CNS1 and CNS3 of the *Foxp3* gene in Treg cells, but not to the region at 1 kb upstream of *Zbtb7b* (*Th-POK*) exon Ia (UP1), which was used as a negative control locus (Setoguchi et al., 2008) (Figure 5B, right). In CNS1 and CNS3, but not in CNS2, there are conserved Runx-binding consensus sites (ACCACA) (Figure S7 and S8), suggesting that the Runx complex might bind to CNS2 via associating with other molecules.

Because *Cbfb*-deleted Treg cells showed IL-4 hyperproduction without overexpression of *Gata3*, we investigated how the Runx complex controlled *Il4* expression in Treg cells. By promoter tiling array analysis, we could not detect the binding of the Runx complex to the *Il4* promoter region in Treg cells. However, by coupling ChIP assay with custom tiling array for the Th2 cytokine locus (~200 base intervals), we found that the Runx complex bound to the *Il4* silencer in Treg cells (Figure 5C, left). We further confirmed this binding by conventional ChIP assays (Figure 5C, right). Thus, the Runx complex may repress *Il4* expression in Treg cells via binding to the *Il4* silencer as in naive CD4$^+$ T cells and Th1 cells, as we and others have recently reported (Djuretic et al., 2007; Naoe et al., 2007). ChIP and promoter tiling array also revealed that the Runx complex bound to the promoter region of the *Ifng* gene in Treg cells, being consistent with our previous finding that Runx1 bound to this region (Ono et al., 2007) (Figure S9). The Runx complex also bound to the regulatory region of the *Gzmb* gene, which is highly expressed in Treg cells in specific environment and is involved in Treg cell-suppressive function (Cao et al., 2007; Gondek et al., 2005) (Figure S10). Thus, the Runx complex binds

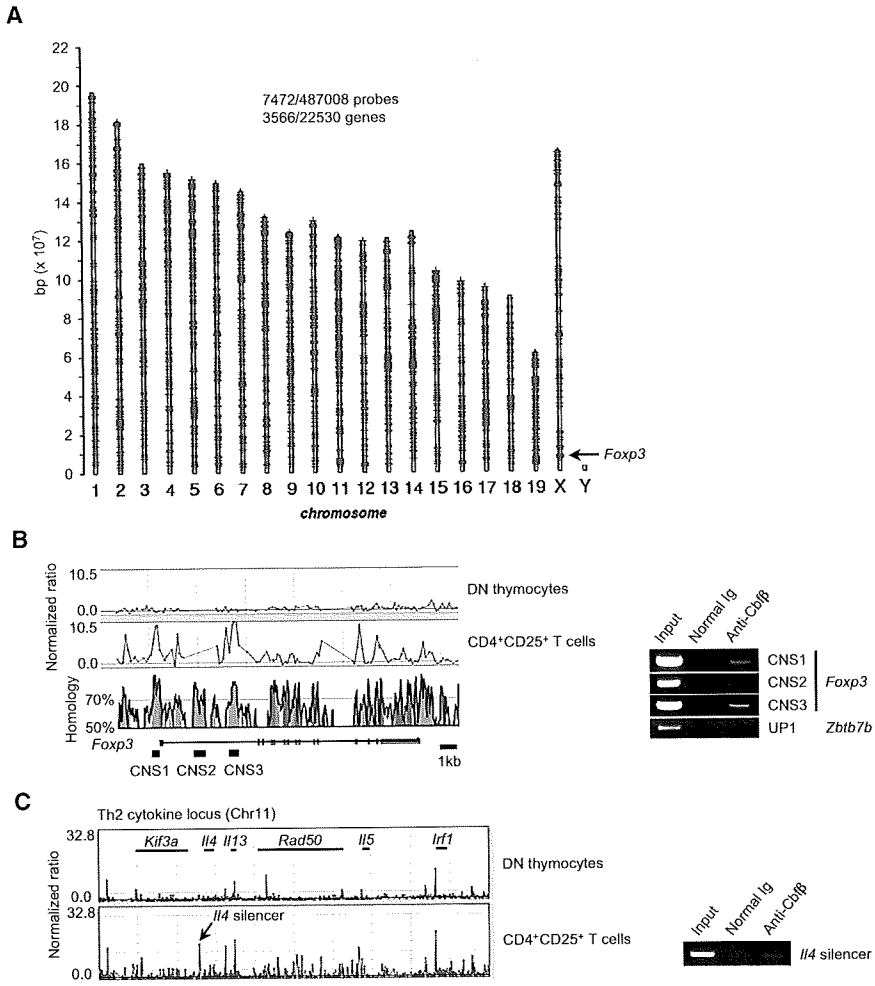

Figure 5. Binding of the Runx Complex to Regulatory Regions of *Foxp3* and *Il4*

(A) The Runx complex bound to promoter regions of various genes in Treg cells. MACS-purified $CD4^+CD25^+$ T cells of wild-type BALB/c mice were subjected to ChIP with anti-Cbfβ followed by promoter tiling array. Red crosses indicate Cbfβ-bound genes.

(B) The Runx complex bound to CNSs of the *Foxp3* gene in Treg cells of BALB/c mice. The binding of the Runx complex to the *Foxp3* gene locus in double negative (DN) thymocytes and peripheral $CD4^+CD25^+$ T cells from BALB/c mice was examined through a custom tiling array for the *Foxp3* locus coupled with ChIP with Cbfβ antibody (left). The signal intensity value of an individual probe is represented by a red dot in correspondence to the structure of the mouse *Foxp3* gene and mouse-human VISTA homology plot of the *Foxp3* gene. Red areas and blue areas in the VISTA plot indicate highly homologous regions and the exons of the mouse *Foxp3* gene, respectively. Gray squares in the figure of *Foxp3* gene structure indicate 5′ untranslated regions (UTRs). The binding of the Runx complex to CNSs of the *Foxp3* gene and the UP1 region of the *Zbtb7b* gene was assessed by conventional ChIP assays (right).

(C) The Runx complex bound to the *Il4* silencer in Treg cells of BALB/c mice. The binding of the Runx complex to the *Il4* silencer in $CD4^+CD25^+$ T cells from BALB/c mice was detected with the combination of ChIP and genome tiling array customized for Th2 cytokine locus (left) and conventional ChIP assays (right).

to the regulatory regions of *Foxp3*, *Il4*, and other genes in Treg cells.

RUNX1 Is Required for Optimal Regulation of FoxP3 Expression

The decreased FoxP3 expression in *Cbfb*-deleted Treg cells suggests that the Runx complex is required for constitutive FoxP3 expression in Treg cells. Because introduction of siRNA against *RUNX1* into human Treg cells efficiently repressed *RUNX1* expression (Ono et al., 2007), we examined the effect of *RUNX1* knockdown on FoxP3 expression in FoxP3-expressing T cell line MT-2 and in primary human $CD4^+CD25^{hi}$ cells. Both MT-2 cells and human Treg cells showed attenuated expression of FoxP3 after *RUNX1* siRNA transfection, indicating a key contribution of RUNX1 to the maintenance of constitutive FoxP3 expression (Figure 6A). Even in the presence of 100 U/ml of IL-2, Treg cells transduced with *RUNX1* siRNA still showed lower FoxP3 expression, indicating that attenuated FoxP3 expression was independent of IL-2 supply (Figure 6B). Further, by RT-PCR, *FOXP3* mRNA expression was slightly but significantly decreased in *Cbfb*-deleted Treg cells and *RUNX1* siRNA-introduced MT-2 cells, indicating that the Runx complex regulated FoxP3 expression, at least in part, at the level of transcription (Figure S6 and Figure 6C). Moreover, with human primary naive $CD4^+$ T cells, in which T cell receptor (TCR) stimulation can induce FoxP3 expression (Mantel et al., 2006; Walker et al., 2003), *RUNX1* knockdown attenuated this activation-induced FoxP3 expression (Figure 6D). This suggests that the Runx complex controls not only constitutive expression of FoxP3 in natural Treg cells but also its de novo induction in activated human $CD4^+$ T cells.

Given that the Runx complex binds to the possible regulatory regions of the *FOXP3* gene, it may directly control *FOXP3* transcription in Treg cells. We thus assessed the direct contribution of the Runx complex to *FOXP3* transcription by reporter gene assays. CNS1 and CNS3 of the human *FOXP3* gene exhibited significant transactivational activities in $CD4^+$ T cells (Figure S11A and Supplemental Data). The mutations of Runx-binding sites in the CNS1 and CNS3 constructs failed to attenuate the transactivational activities observed in those constructs (Figure S11B and Supplemental Data). However, the Runx-site mutations in CNS1 abrogated the transactivation of the construct in response to the stimulation (Figure 6E, left). In contrast to CNS1, the CNS3 construct, either of wild-type or mutant, showed no response to the stimulation (Figure 6E, right). Similar results were also observed in FoxP3-expressing ATL-43T, a human adult T cell leukemia cell line (Figure 6F).

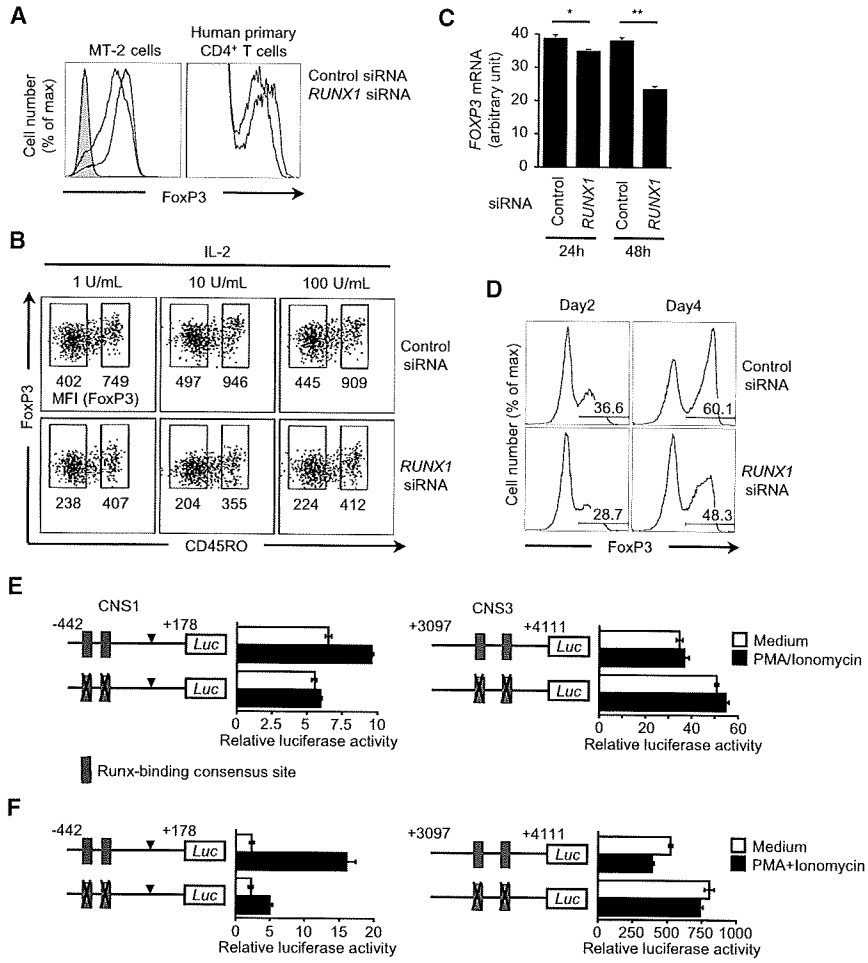

Figure 6. RUNX1 Was Required for Optimal Regulation of FoxP3 Expression

(A) Expression of FoxP3 by MT-2 cells and human primary CD4$^+$ T cells transduced with control or *RUNX1* siRNA 3 days and 4 days after transduction, respectively. Results representative of three experiments are shown.

(B) Effect of exogenous IL-2 on FoxP3 expression by human primary CD4$^+$CD25^{hi}CD45RO$^-$ naive Treg cells and CD4$^+$CD25^{hi}CD45RO$^+$ memory Treg cells transduced with control or *RUNX1* siRNA. siRNA-transduced human Treg cells were purified 24 hr after transduction; this process was followed by culture for 3 days in the presence of the indicated concentrations of exogenous IL-2. Numbers shown below the gates indicate the mean fluorescence intensity (MFI) of FoxP3 in the gates. Data are representative of two experiments.

(C) Relative mRNA expression of *FOXP3* in MT-2 cells transduced with control or *RUNX1* siRNA 24 hr and 48 hr after transduction. RNA was extracted from purified PI (propidium iodide)-negative viable MT-2 cells. Results of three experiments are shown as the mean ± SD values. *p = 0.01; **p = 0.0001 (unpaired t test).

(D) *RUNX1* knockdown attenuated activation-induced FoxP3 expression in human primary naive CD4$^+$ T cells. siRNA-introduced CD4$^+$CD25$^-$ CD45RO$^-$ naive T cells were stimulated with anti-CD3 and anti-CD28 in the presence of antigen-presenting cells for 2 or 4 days. Numbers shown above the gates indicate the percentages of CD4$^+$FoxP3$^+$ cells in CD4$^+$ T cells. Results representative of two experiments are shown.

(E and F) Activation of the *FOXP3* CNS1 by stimulation with PMA and ionomycin is dependent on Runx-binding consensus sequences. The *FOXP3* CNS1 and CNS3 constructs with or without mutations in Runx sites were transfected into human primary CD4$^+$ T cells (E) and ATL 43T cells (F) and cultured in medium or in medium containing PMA and ionomycin. Results shown are the mean ± SD of triplicates done in one experiment representative of three.

Taken together, these results suggest that the Runx complex is required for optimal regulation of FoxP3 expression.

Analyses of *Runx1$^{F/F}$: FIC* and *Runx3$^{F/F}$: FIC* Mice

Because both Runx1 and Runx3 were expressed in Treg cells (Figure S12; Ono et al., 2007), we next investigated which one played a key role for Treg cell function in vivo. We generated *Runx1$^{F/F}$: FIC* and *Runx3$^{F/F}$: FIC* mice by crossing *FIC* mice with *Runx1*-floxed or *Runx3*-floxed mice, respectively (Naoe et al., 2007; Taniuchi et al., 2002). *Runx1$^{F/F}$: FIC* mice developed histologically evident gastritis, high titers of parietal cell antibodies, and hyperproduction of IgE as observed in *Cbfb$^{F/F}$: FIC* mice, whereas IgG production was not significantly altered (Figures 7A–7D). By contrast, *Runx3$^{F/F}$: FIC* mice did not develop gastritis, parietal cell antibodies, or hyperproduction of IgE (Figures 7B–7D). *Runx1*- but not *Runx3*-deleted Treg cells showed attenuated FoxP3 expression as observed in *Cbfb*-deleted Treg cells (Figure 7E). In addition, *Runx1*- or *Runx3*-deleted Treg cells did not lose CD103 expression, whereas *Cbfb*-deleted Treg cells lost it, indicating that Runx1 and Runx3 function redundantly in the regulation of CD103 expression (Figure 7F). Also, the finding indicates that autoimmune phenotypes due to Cbfβ deficiency in Treg cells is not attributed to the loss of CD103 expression because CD103 expression was not altered in autoimmune *Runx1$^{F/F}$: FIC* mice. Our results thus demonstrate that Runx1, but not Runx3, is indispensable for in vivo Treg cell function but do not exclude possible functional compensation between Runx1 and Runx3 in Treg cells.

DISCUSSION

In this study, we showed that Treg cell-specific deficiency of Cbfβ or Runx1, but not Runx3, impaired in vivo Treg cell function, resulting in the development of autoimmune disease and hyperproduction of IgE. The immunological diseases were similar in spectrum to those found in FoxP3 mutant or -deficient mice, although the disease severities were much milder (Sakaguchi et al., 2006).

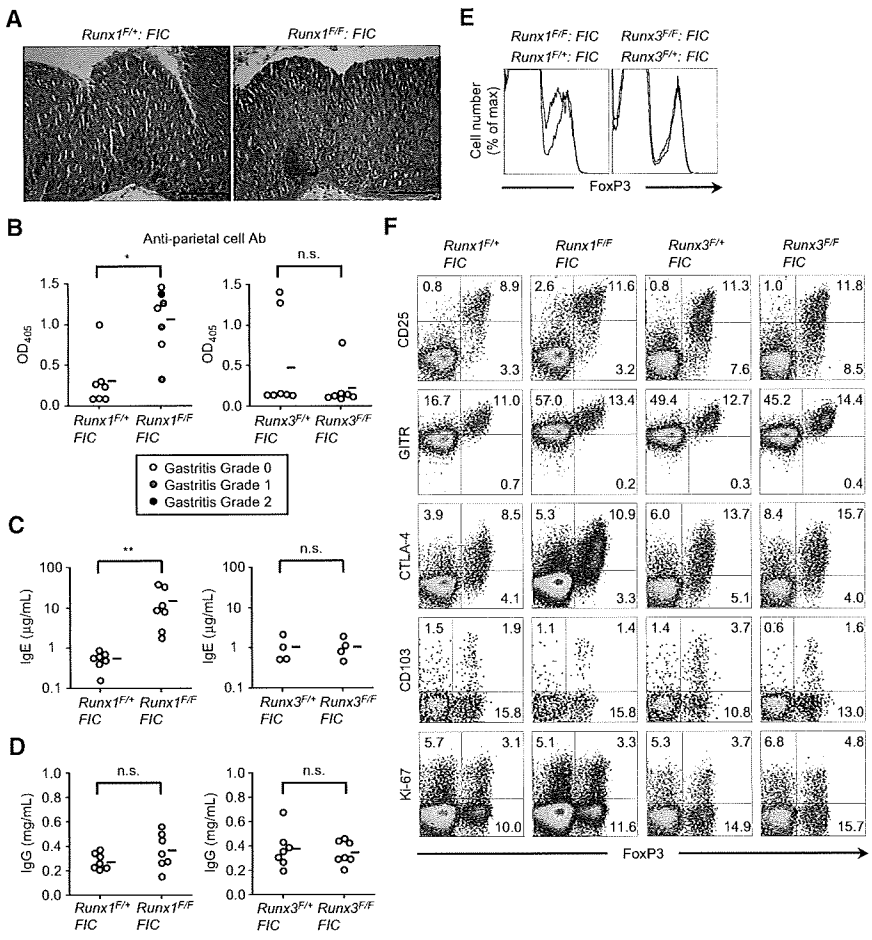

Figure 7. Development of Autoimmune Disease and Hyperproduction of IgE in *Runx1$^{F/F}$: FIC* Mice, but Not in *Runx3$^{F/F}$: FIC* Mice

(A) Hematoxylin and eosin staining of stomach sections of 8- to 9-week-old *Runx1$^{F/F}$: FIC* and *Runx1$^{F/+}$: FIC* littermates (n = 7). Representative photomicrographs are shown. Scale bars represent 10.0 μm.

(B) Titers of parietal cell autoantibodies in the sera of 8- to 9-week-old *Runx1$^{F/F}$: FIC* and *Runx1$^{F/+}$: FIC* littermates (n = 7) (left) and *Runx3$^{F/F}$: FIC* and *Runx3$^{F/+}$: FIC* littermates (n = 7) (right) were assessed by ELISA. Horizontal lines represent averages from each group. *p = 0.01.

(C and D) Titers of IgE (C) and IgG (D) in the sera of 8- to 9-week-old *Runx1$^{F/F}$: FIC* and *Runx1$^{F/+}$: FIC* littermates (n = 7) and *Runx3$^{F/F}$: FIC* and *Runx3$^{F/+}$: FIC* littermates (n = 4) were assessed by ELISA. Horizontal lines represent averages from each group. **p = 0.002.

(E) Flow cytometric analysis of FoxP3 expression by CD4$^+$ T cells from *Runx1$^{F/F}$: FIC* and *Runx1$^{F/+}$: FIC* littermates (left) and from *Runx3$^{F/F}$: FIC* and *Runx3$^{F/+}$: FIC* littermates (right) at 7 weeks of age. Results representative of three experiments are shown.

(F) Expression of FoxP3 and the indicated molecules by *Runx1$^{F/F}$: FIC* and *Runx1$^{F/+}$: FIC* littermates and by *Runx3$^{F/F}$: FIC* and *Runx3$^{F/+}$: FIC* littermates at 7 to 10 weeks of age. Results representative of three experiments are shown.

We have previously shown that Runx1 binds to the promoter of the *Il2* and *Ifng* genes and enhances IL-2 and IFN-γ production in conventional T cells. Conversely, the FoxP3-Runx1 complex, together with other transcription factors such as NFAT, represses the expression of these cytokines and confers in vitro-suppressive activity to Treg cells (Ono et al., 2007). Here, we have provided genetic evidence that Treg cell-specific deficiency of the Runx1-Cbfβ complex indeed impairs in vivo Treg cell function. This indicates that Runx-dependent gene regulation is critically required for in vivo Treg cell function. In addition, Cbfβ-deficient Treg cells transcribed *Il17a* and *Rorgt* to lesser extents than control Treg cells, whereas *Il4*, *Il10*, and *Tbx21* increased in the former. Other studies have shown that Runx1 induces the expression of RORγt, interacts with RORγt in conventional T cells, and regulates *Il17* transcription via controlling the promoter or enhancer regions of the *Il17* gene (Zhang et al., 2008). Runx3 also acts with T-bet to activate *Ifng* and silence *Il4* via binding to the *Ifng* promoter and the *Il4* silencer regions, respectively, leading to Th1 cell-specific cytokine production (Djuretic et al., 2007). Further, Runx1 and Runx3 interact with the *Cd4* silencer and the *Zbtb7b* silencer, in regulating thymocyte commitment to the CD8$^+$ T cell lineage by repressing the alternative cell fate (Setoguchi et al., 2008; Taniuchi et al., 2002). Thus, the Runx complex plays critical roles not only in T cell differentiation, in particular CD4-CD8 lineage commitment, but also in conferring a variety of functions to T cell subsets including Th1, Th17, and Treg cell. Further, phenotypical differences between *Runx1*- and *Runx3*-deleted Treg cells suggest that Runx1 and Runx3 differently contribute to the differentiation and the functions of T cell subsets. The Runx complex may thus function as an essential core transcriptional "modifier" to regulate specialized effector functions of CD4$^+$ T cell subsets by associating with particular lineage-specific transcription factors including FoxP3.

Regarding the mechanism by which Treg cell function is impaired in Cbfβ- or Runx1-deficient Treg cells, a notable finding is that Cbfβ or Runx1 deficiency accompanies attenuated expression of FoxP3 at mRNA and protein levels. Because attenuated FoxP3 expression can lead to loss of Treg cell-suppressive function, as demonstrated by others (Wan and Flavell, 2007), reduced expression of FoxP3 might be responsible for dysfunction of *Cbfb*-deleted Treg cells. For example, *Nrp1* and *Pde3b*, which were differentially expressed in *Cbfb*-deleted Treg cells by expression microarray, could be affected by FoxP3 hypoexpression. Other differentially expressed genes are also possibly associated with the impaired function of *Cbfb*-deleted Treg cells. They include *Il4*, *Ltb4r1*, *Cd160*, and *Ccr5*, all of which were overexpressed in *Cbfb*-deleted Treg cells. Of particular note is the hyperproduction of IL-4 by *Cbfb*-deleted Treg cells. Elevated IL-4 may contribute to the impaired Treg cell-mediated suppression in *Cbfb*- or *Runx1*-deleted Treg

cells because it has been shown that the addition of exogenous IL-4 renders $CD4^+CD25^-$ conventional T cells resistant to in vitro Treg cell-mediated suppression (Pace et al., 2006). We and others have previously reported that the Runx complex represses *Il4* via binding to the *Il4* silencer in naive $CD4^+$ T cells and Th1 cells (Djuretic et al., 2007; Naoe et al., 2007). Our observation that the Runx complex bound to the *Il4* silencer in Treg cells suggests that the complex similarly represses *Il4* expression in Treg cells and that loss of Runx complex derepresses *Il4*, leading to hyperproduction of IL-4 in *Cbfb*-deleted Treg cells. Nonetheless, it is also possible that reduction of FoxP3 expression directly derepresses *Il4* expression. Taken together, our findings show that impaired suppressive function of *Cbfb*-deleted Treg cells could be attributed, at least in part, to the reduction of FoxP3 and the hyperproduction of IL-4, in addition to the impaired formation of the Runx-Cbfβ-FoxP3 complex (Ono et al., 2007).

The maintenance of constitutive FoxP3 expression in Treg cells appears to require the Runx complex. Our observations that the complex bound to the regulatory regions of the *Foxp3* gene in Treg cells may suggest that the Runx complex would directly upregulate FoxP3 expression. In the reporter assays, however, Runx-binding site-dependent transactivation was observed only under activated condition, and not under unstimulated condition. This suggests that the Runx complex regulates constitutive FoxP3 expression more than by transactivating the *FOXP3* gene. It has also been shown that RUNX1 not only is a conventional transcriptional activator but also plays a critical role in chromatin modifications such as histone acetylation via interacting with histone acetyltransferases (Yoshida and Kitabayashi, 2008). This suggests that the binding of the Runx complex to the *Foxp3* gene regulatory regions may contribute to constitutive FoxP3 expression through epigenetic regulation. It is also possible that the deficiency of the Runx complex may primarily dysregulate other genes encoding molecules necessary for the maintenance of FoxP3 expression in Treg cells. These possibilities are currently under investigation.

Our results support the concept that Runx-dependent program plays essential roles for immune homeostasis including Treg cell-mediated immune suppression. Single-nucleotide polymorphisms (SNPs) affecting the consensus sites for RUNX1 are associated with the genetic susceptibility to several autoimmune diseases including systemic lupus erythematosus, rheumatoid arthritis, and psoriasis (Alarcon-Riquelme, 2004; Helms et al., 2003; Prokunina et al., 2002; Tokuhiro et al., 2003). In addition, a SNP in the *RUNX1* gene itself was strongly associated with rheumatoid arthritis (Tokuhiro et al., 2003). It is thus likely that genetic alterations of *RUNX1* may contribute to the development of autoimmune diseases in part by means of affecting Treg cell-mediated immune regulation. Furthermore, our study suggests that Treg cell-specific inhibition of the activity of the Runx1-Cbfβ complex could be useful for reducing Treg cell activity and thereby evoking effective tumor immunity.

EXPERIMENTAL PROCEDURES

Mice

C.B-17 SCID mice were purchased from CLEA Japan (Tokyo, Japan). BALB/c mice were purchased from Japan SLC (Shizuoka, Japan). *Foxp3-Ires-Cre (FIC)*, $Runx1^F$, $Runx3^F$, and $Cbfb^F$ mouse strains were described previously (Naoe et al., 2007; Taniuchi et al., 2002; Wing et al., 2008). In this paper, a mouse described with a "*FIC*" genotype was either a *FIC/Y* hemizygote male or *FIC/FIC* homozygote female. All mice were maintained in our animal facility and treated in accordance with the guidelines for animal care approved by the Institute for Frontier Medical Sciences, Kyoto University.

Antibodies

Biotinylated or FITC-, phycoerythrin (PE)-, PerCP-Cy5.5-, or allophycocyanin (APC)-conjugated mAbs for CD4, CD8, CD25, HSA (CD24), TCRβ, CD69, CD122, CD44, CD62L, CTLA-4, Ki-67, CD127, CD103, IFN-γ, IL-2, IL-4, IL-10, and IL-17 were purchased from BD Biosciences. Biotinylated anti-GITR (DTA1) was previously described (Shimizu et al., 2002). APC-conjugated anti-mouse Foxp3 (FJK-16 s) was purchased from eBioscience. The following mAbs were used for detecting human antigens: PerCP-Cy5.5-conjugated anti-CD4 and FITC-conjugated anti-CD45RO from BD Biosciences and biotinylated anti-human FOXP3 (236A/E7) from eBiosciences. Cbfβ antibody was generated by immunizing rabbits with peptides corresponding to the N-terminal of Cbfβ.

Histology

Gastritis and colitis were graded in a blinded fashion in accordance with the published criteria (Asano et al., 1996; Asseman et al., 1999).

Immunoblotting

Lysates prepared from purified 5×10^3 cells were loaded and immunoblotted with anti-Cbfβ.

Identification of $Cbfb^F$ and *Cbfb*-Deleted Allele by PCR

Equivalent amounts of genomic DNA extracted from individual lymphocyte subset were subjected to multiplex PCR with the following primers: G2, 5′-CCTCCTCATTCTAACAGGAATC-3′; G3, 5′-GGTTAGGAGTCATTGTGATC AC-3′; and G6, 5′-CATTGGATTGGCGTTACTGG-3′. $Cbfb^F$ and *Cbfb*-deleted alleles were identified by PCR amplification with the G3/G2 and the G3/G6 primer pair, respectively (Figure S13). The $Cbfb^F$ allele-specific and the *Cbfb*-deleted allele-specific amplicons were distinguished according to their length.

ELISA

Autoantibodies specific for gastric parietal cells were detected by ELISA as previously described (Sakaguchi et al., 1995). Serum IgG and IgE levels were assessed by ELISA with Mouse IgG ELISA Quantitation Kit (Bethyl Laboratories) and OptEIA Mouse IgE ELISA set (BD Biosciences), respectively.

Cell Sorting

Fresh mouse $CD4^+$ T cells were isolated as previously described (Hori et al., 2003). Then, $CD4^+$ T cell subpopulations including $CD4^+CD25^{hi}$ cells, $CD4^+CD25^-$ cells, and $CD4^+CD25^-CD45RB^{hi}$ cells were purified by sorting with a cell sorter (MoFlo, Dako). In some experiments, $CD4^+CD25^+$ cells were purified by MACS (Miltenyi Biotec).

Intracellular Cytokine Staining

Cells were stimulated for 5 hr with 20 ng/ml phorbol 12-myristate 13-acetate (PMA) and 1 μM ionomycin in the presence of GolgiStop (BD Biosciences). For intracellular cytokine staining, stimulated cells were stained for surface antigens, fixed, permeabilized with BD Cytofix/Cytoperm (BD Biosciences), and stained by anti-cytokine. For costaining of intracellular cytokine and FoxP3, stimulated cells were stained for surface antigens, fixed, permeabilized with Foxp3 Fixation/Permeabilization Kit (eBioscience), and finally, costained with cytokine antibody and Foxp3 antibody.

Proliferation Assay and Suppression Assay

A total of 2×10^4 responder T cells were cultured with or without graded numbers of suppressor cells for 3 days in the presence of 4×10^4 antigen-presenting cells (mitomycin C-treated $Thy1.2^+$ cell-depleted BALB/c splenocytes) and 0.5 μg/ml CD3 antibody (145-2C11, BD Biosciences). [^{3}H]thymidine (1 μCi/well) was added during the last 8 hr of culture.

Quantitative Real-Time RT-PCR

Total RNA was prepared from cells of interest with RNeasy Mini Kit (QIAGEN). cDNA was synthesized from total RNA with SuperScript III reverse transcriptase and oligo(dT)$_{12-18}$ primer (Invitrogen). Quantitative real-time RT-PCR was performed with the LightCycler 480 System (Roche Applied Science) with QuantiTect SYBR Green PCR Kit (QIAGEN). Primer pairs used are listed in Table S4. All samples were run in triplicate and the data were normalized to *Hprt* mRNA expression.

Chromatin Immunoprecipitation and Tiling Array

Cells were crosslinked by the addition of one-tenth volume of fresh 11% formaldehyde solution for 10 min at room temperature. Cells were resuspended, lysed in lysis buffers, and sonicated for solubilization and shearing of crosslinked DNA. The cell extract was incubated overnight at 4°C with 100 μl of Dynal anti-rabbit IgG magnetic beads that had been preincubated with 10 μg of the Cbfβ antibody. Beads were washed five times with RIPA buffer and one time with TE containing 50 mM NaCl. Bound complexes were eluted from the beads by heating at 65°C with occasional vortexing, and crosslinking was reversed by overnight incubation at 65°C. Immunoprecipitated DNA and whole-cell extract DNA were then purified by treatment with RNaseA, proteinase K, and multiple phenol:chloroform:isoamyl alcohol extractions. For conventional ChIP assays, the precipitated DNA was subjected to PCR amplification. The primers used are as follows: FxCNS1-for, 5′-AGCCCTGT TATCTCATTGATAC-3′; FxCNS1-rev, 5′-GACCTCGCTCTTCTAATAATCC-3′; FxCNS2-for, 5′-CCCATACCCACACTTTTGACCTCTG-3′; FxCNS2-rev, 5′-GC ACTTGAAAATGAGATAACTGTTCA-3′; FxCNS3-for, 5′-CTGGCATCCAAGAA AGACA-3′; and FxCNS3-rev, 5′-GGCTTCATCGGCAACAA-3′. Primers for *Il4* silencer region and for the region at 1 kb upstream of *Zbtb7b* (*Th-POK*) exon Ia (UP1) were described previously (Naoe et al., 2007; Setoguchi et al., 2008). For a ChIP-on-chip experiment, purified DNA was amplified twice by LM-PCR in accordance with the manufacturer's protocol (Agilent). We used mouse promoter array and custom microarrays generated by Agilent that tiled through several loci via 60-nucleotide oligonucleotide probes. The probes, representing the forward strand, were spaced every 200 bases and were printed at random location on the array. Probe hybridization and scanning of oligonucleotide array data were performed in accordance with the manufacturer's protocol (Agilent). Data analyses were carried out with Feature Extraction software and ChIP Analytics software (Agilent).

RNA Interference

MT-2 cells and MACS-sorted primary human CD4$^+$ T cells were transduced with *RUNX1* siRNA (HSS141472; Invitrogen) or Stealth RNAi negative control GC high (Invitrogen) as previously described (Ono et al., 2007).

Expression Microarray

Total RNA was isolated with the RNeasy Micro Kit (QIAGEN). Biotinylated antisense cRNA was prepared by two cycles of in vitro amplication. Biotinylated cRNA (15 μg) was hybridized to Affymetrix GeneChip Mouse Genome 430 2.0 arrays. Data analyses were done with the use of MeV (v4.2) (Saeed et al., 2003).

Induction of FoxP3 Expression in Human Naive T Cells

CD25$^-$CD45RO$^-$ primary human naive T cells were negatively sorted with MACS Pan T Cell Isolation Kit II, CD25 MicroBeads, and CD45RO MicroBeads (Miltenyi Biotec). A total of 7 × 10^6 purified naive T cells were transduced with control or *RUNX1* siRNA with a Human T Cell Nucleofector Kit (Amaxa), mixed with 4 × 10^6 T cell-depleted syngeneic PBMCs, and then cultured in a volume of 1 ml (12-well plates) for 24 h. Then, 7 × 10^5 cells were harvested and cultured in a volume of 200 μl (96-well plates) in the presence of 0.01 μg/ml anti-CD3 (OKT3) and 0.02 μg/ml anti-CD28 (CD28.2) for 4 days. Blood samples were obtained from healthy adult volunteers (20–40 years old). The study was conducted with the approval from the human ethics committee of the Institute for Frontier Medical Sciences, Kyoto University.

Statistical analysis

Comparisons were analyzed for statistical significance by Mann-Whitney U test, unless otherwise stated, with $p < 0.05$ being considered significant.

ACCESSION NUMBERS

Microarray data are available from the National Center for Biotechnology Information Gene Expression Omnibus (GEO) under accession number GSE18148.

SUPPLEMENTAL DATA

Supplemental Data include 13 figures, 5 tables, and Supplemental Experimental Procedures and can be found with this article online at http://www.cell.com/immunity/supplemental/S1074-7613(09)00407-5.

ACKNOWLEDGMENTS

We thank M. Kakino, R. Ishii, M. Yoshida, and K. Akiyama for technical assistance; M. Matsuoka for ATL-43T cell line; and M. Matsushita for preparing histology.

Received: August 24, 2009
Revised: September 9, 2009
Accepted: September 14, 2009
Published online: October 1, 2009

REFERENCES

Alarcon-Riquelme, M.E. (2004). Role of RUNX in autoimmune diseases linking rheumatoid arthritis, psoriasis and lupus. Arthritis Res. Ther. *6*, 169–173.

Annacker, O., Coombes, J.L., Malmstrom, V., Uhlig, H.H., Bourne, T., Johansson-Lindbom, B., Agace, W.W., Parker, C.M., and Powrie, F. (2005). Essential role for CD103 in the T cell-mediated regulation of experimental colitis. J. Exp. Med. *202*, 1051–1061.

Asano, M., Toda, M., Sakaguchi, N., and Sakaguchi, S. (1996). Autoimmune disease as a consequence of developmental abnormality of a T cell subpopulation. J. Exp. Med. *184*, 387–396.

Asseman, C., Mauze, S., Leach, M.W., Coffman, R.L., and Powrie, F. (1999). An essential role for interleukin 10 in the function of regulatory T cells that inhibit intestinal inflammation. J. Exp. Med. *190*, 995–1004.

Bettelli, E., Dastrange, M., and Oukka, M. (2005). Foxp3 interacts with nuclear factor of activated T cells and NF-kappa B to repress cytokine gene expression and effector functions of T helper cells. Proc. Natl. Acad. Sci. USA *102*, 5138–5143.

Cao, X., Cai, S.F., Fehniger, T.A., Song, J., Collins, L.I., Piwnica-Worms, D.R., and Ley, T.J. (2007). Granzyme B and perforin are important for regulatory T cell-mediated suppression of tumor clearance. Immunity *27*, 635–646.

de Bruijn, M.F., and Speck, N.A. (2004). Core-binding factors in hematopoiesis and immune function. Oncogene *23*, 4238–4248.

Djuretic, I.M., Levanon, D., Negreanu, V., Groner, Y., Rao, A., and Ansel, K.M. (2007). Transcription factors T-bet and Runx3 cooperate to activate Ifng and silence Il4 in T helper type 1 cells. Nat. Immunol. *8*, 145–153.

Durst, K.L., and Hiebert, S.W. (2004). Role of RUNX family members in transcriptional repression and gene silencing. Oncogene *23*, 4220–4224.

Egawa, T., Tillman, R.E., Naoe, Y., Taniuchi, I., and Littman, D.R. (2007). The role of the Runx transcription factors in thymocyte differentiation and in homeostasis of naive T cells. J. Exp. Med. *204*, 1945–1957.

Fontenot, J.D., Gavin, M.A., and Rudensky, A.Y. (2003). Foxp3 programs the development and function of CD4+CD25+ regulatory T cells. Nat. Immunol. *4*, 330–336.

Gondek, D.C., Lu, L.F., Quezada, S.A., Sakaguchi, S., and Noelle, R.J. (2005). Cutting edge: Contact-mediated suppression by CD4+CD25+ regulatory cells involves a granzyme B-dependent, perforin-independent mechanism. J. Immunol. *174*, 1783–1786.

Grueter, B., Petter, M., Egawa, T., Laule-Kilian, K., Aldrian, C.J., Wuerch, A., Ludwig, Y., Fukuyama, H., Wardemann, H., Waldschuetz, R., et al. (2005). Runx3 regulates integrin alpha E/CD103 and CD4 expression during development of CD4-/CD8+ T cells. J. Immunol. *175*, 1694–1705.

Helms, C., Cao, L., Krueger, J.G., Wijsman, E.M., Chamian, F., Gordon, D., Heffernan, M., Daw, J.A., Robarge, J., Ott, J., et al. (2003). A putative RUNX1 binding site variant between SLC9A3R1 and NAT9 is associated with susceptibility to psoriasis. Nat. Genet. *35*, 349–356.

Hill, J.A., Feuerer, M., Tash, K., Haxhinasto, S., Perez, J., Melamed, R., Mathis, D., and Benoist, C. (2007). Foxp3 transcription-factor-dependent and -independent regulation of the regulatory T cell transcriptional signature. Immunity *27*, 786–800.

Hori, S., Nomura, T., and Sakaguchi, S. (2003). Control of regulatory T cell development by the transcription factor Foxp3. Science *299*, 1057–1061.

Khattri, R., Cox, T., Yasayko, S.A., and Ramsdell, F. (2003). An essential role for Scurfin in CD4+CD25+ T regulatory cells. Nat. Immunol. *4*, 337–342.

Kim, H.P., and Leonard, W.J. (2007). CREB/ATF-dependent T cell receptor-induced FoxP3 gene expression: A role for DNA methylation. J. Exp. Med. *204*, 1543–1551.

Komine, O., Hayashi, K., Natsume, W., Watanabe, T., Seki, Y., Seki, N., Yagi, R., Sukzuki, W., Tamauchi, H., Hozumi, K., et al. (2003). The Runx1 transcription factor inhibits the differentiation of naive CD4+ T cells into the Th2 lineage by repressing GATA3 expression. J. Exp. Med. *198*, 51–61.

Li, B., Samanta, A., Song, X., Iacono, K.T., Bembas, K., Tao, R., Basu, S., Riley, J.L., Hancock, W.W., Shen, Y., et al. (2007). FOXP3 interactions with histone acetyltransferase and class II histone deacetylases are required for repression. Proc. Natl. Acad. Sci. USA *104*, 4571–4576.

Mantel, P.Y., Ouaked, N., Ruckert, B., Karagiannidis, C., Welz, R., Blaser, K., and Schmidt-Weber, C.B. (2006). Molecular mechanisms underlying FOXP3 induction in human T cells. J. Immunol. *176*, 3593–3602.

Naoe, Y., Setoguchi, R., Akiyama, K., Muroi, S., Kuroda, M., Hatam, F., Littman, D.R., and Taniuchi, I. (2007). Repression of interleukin-4 in T helper type 1 cells by Runx/Cbf beta binding to the Il4 silencer. J. Exp. Med. *204*, 1749–1755.

Ochs, H.D., Ziegler, S.F., and Torgerson, T.R. (2005). FOXP3 acts as a rheostat of the immune response. Immunol. Rev. *203*, 156–164.

Ono, M., Yaguchi, H., Ohkura, N., Kitabayashi, I., Nagamura, Y., Nomura, T., Miyachi, Y., Tsukada, T., and Sakaguchi, S. (2007). Foxp3 controls regulatory T-cell function by interacting with AML1/Runx1. Nature *446*, 685–689.

Pace, L., Rizzo, S., Palombi, C., Brombacher, F., and Doria, G. (2006). Cutting edge: IL-4-induced protection of CD4+CD25- Th cells from CD4+CD25+ regulatory T cell-mediated suppression. J. Immunol. *176*, 3900–3904.

Prokunina, L., Castillejo-Lopez, C., Oberg, F., Gunnarsson, I., Berg, L., Magnusson, V., Brookes, A.J., Tentler, D., Kristjansdottir, H., Grondal, G., et al. (2002). A regulatory polymorphism in PDCD1 is associated with susceptibility to systemic lupus erythematosus in humans. Nat. Genet. *32*, 666–669.

Saeed, A.I., Sharov, V., White, J., Li, J., Liang, W., Bhagabati, N., Braisted, J., Klapa, M., Currier, T., Thiagarajan, M., et al. (2003). TM4: A free, open-source system for microarray data management and analysis. Biotechniques *34*, 374–378.

Sakaguchi, S., Ono, M., Setoguchi, R., Yagi, H., Hori, S., Fehervari, Z., Shimizu, J., Takahashi, T., and Nomura, T. (2006). Foxp3+ CD25+ CD4+ natural regulatory T cells in dominant self-tolerance and autoimmune disease. Immunol. Rev. *212*, 8–27.

Sakaguchi, S., Sakaguchi, N., Asano, M., Itoh, M., and Toda, M. (1995). Immunologic self-tolerance maintained by activated T cells expressing IL-2 receptor alpha-chains (CD25). Breakdown of a single mechanism of self-tolerance causes various autoimmune diseases. J. Immunol. *155*, 1151–1164.

Sato, T., Ohno, S., Hayashi, T., Sato, C., Kohu, K., Satake, M., and Habu, S. (2005). Dual functions of Runx proteins for reactivating CD8 and silencing CD4 at the commitment process into CD8 thymocytes. Immunity *22*, 317–328.

Setoguchi, R., Tachibana, M., Naoe, Y., Muroi, S., Akiyama, K., Tezuka, C., Okuda, T., and Taniuchi, I. (2008). Repression of the transcription factor Th-POK by Runx complexes in cytotoxic T cell development. Science *319*, 822–825.

Shimizu, J., Yamazaki, S., Takahashi, T., Ishida, Y., and Sakaguchi, S. (2002). Stimulation of CD25(+)CD4(+) regulatory T cells through GITR breaks immunological self-tolerance. Nat. Immunol. *3*, 135–142.

Speck, N.A. (2001). Core binding factor and its role in normal hematopoietic development. Curr. Opin. Hematol. *8*, 192–196.

Taniuchi, I., and Littman, D.R. (2004). Epigenetic gene silencing by Runx proteins. Oncogene *23*, 4341–4345.

Taniuchi, I., Osato, M., Egawa, T., Sunshine, M.J., Bae, S.C., Komori, T., Ito, Y., and Littman, D.R. (2002). Differential requirements for Runx proteins in CD4 repression and epigenetic silencing during T lymphocyte development. Cell *111*, 621–633.

Tokuhiro, S., Yamada, R., Chang, X., Suzuki, A., Kochi, Y., Sawada, T., Suzuki, M., Nagasaki, M., Ohtsuki, M., Ono, M., et al. (2003). An intronic SNP in a RUNX1 binding site of SLC22A4, encoding an organic cation transporter, is associated with rheumatoid arthritis. Nat. Genet. *35*, 341–348.

Tone, Y., Furuuchi, K., Kojima, Y., Tykocinski, M.L., Greene, M.I., and Tone, M. (2008). Smad3 and NFAT cooperate to induce Foxp3 expression through its enhancer. Nat. Immunol. *9*, 194–202.

van Wijnen, A.J., Stein, G.S., Gergen, J.P., Groner, Y., Hiebert, S.W., Ito, Y., Liu, P., Neil, J.C., Ohki, M., and Speck, N. (2004). Nomenclature for Runt-related (RUNX) proteins. Oncogene *23*, 4209–4210.

Walker, M.R., Kasprowicz, D.J., Gersuk, V.H., Benard, A., Van Landeghen, M., Buckner, J.H., and Ziegler, S.F. (2003). Induction of FoxP3 and acquisition of T regulatory activity by stimulated human CD4+CD25- T cells. J. Clin. Invest. *112*, 1437–1443.

Wan, Y.Y., and Flavell, R.A. (2007). Regulatory T-cell functions are subverted and converted owing to attenuated Foxp3 expression. Nature *445*, 766–770.

Wing, K., Onishi, Y., Prieto-Martin, P., Yamaguchi, T., Miyara, M., Fehervari, Z., Nomura, T., and Sakaguchi, S. (2008). CTLA-4 control over Foxp3+ regulatory T cell function. Science *322*, 271–275.

Woolf, E., Xiao, C., Fainaru, O., Lotem, J., Rosen, D., Negreanu, V., Bernstein, Y., Goldenberg, D., Brenner, O., Berke, G., et al. (2003). Runx3 and Runx1 are required for CD8 T cell development during thymopoiesis. Proc. Natl. Acad. Sci. USA *100*, 7731–7736.

Wu, Y., Borde, M., Heissmeyer, V., Feuerer, M., Lapan, A.D., Stroud, J.C., Bates, D.L., Guo, L., Han, A., Ziegler, S.F., et al. (2006). FOXP3 controls regulatory T cell function through cooperation with NFAT. Cell *126*, 375–387.

Yoshida, H., and Kitabayashi, I. (2008). Chromatin regulation by AML1 complex. Int. J. Hematol. *87*, 19–24.

Zhang, F., Meng, G., and Strober, W. (2008). Interactions among the transcription factors Runx1, RORgammat and Foxp3 regulate the differentiation of interleukin 17-producing T cells. Nat. Immunol. *9*, 1297–1306.

secretion (in which the cytokine-containing vesicles are polarized and extrude directly into the synaptic cleft) and multidirectional secretion have been reported[10,11]. In CTLs, IFN-γ seems to follow the constitutive and synaptic modes of secretion, whereas the chemokine CCL5 is released mainly through the regulated secretory pathway, with an initial synaptic and later multidirectional orientation[12] (Fig. 1). The release of cytokines and the exocytosis of cytotoxic granules depend on somewhat different arrays of trafficking proteins, which suggests that the pathways are distinct[11]. However, ASMase-deficient CTLs from LCMV-infected mice have 70% lower secretion of IFN-γ after restimulation with an LCMV peptide, whereas expression of IFN-γ protein in the CTLs and the release of CCL5 are as high as in wild-type CTLs[4]. Herz *et al.* argue that IFN-γ-containing vesicles are much larger than CCL5 secretory vesicles and therefore have a lower spontaneous contractile force, which necessitates the help of ASMase for optimal extrusion (Fig. 1).

The study by Herz *et al.* adds a new level of regulation and complexity to the induction of perforin-dependent cytotoxicity. The results reported raise several questions that should be addressed. Do the findings obtained with mouse $CD8^+$ CTLs also apply to human ($CD8^+$ or $CD4^-CD8^-$) CTLs? Do patients with a milder form of congenital deficiency in ASMase (Niemann-Pick disease, type B) show CTL dysfunction? Is the expression and activity of ASMase subject to immunoregulation in wild-type CTLs? Is the contraction of the secretory granules in other cytotoxic cell types such as natural killer cells or IFN-α/β-producing killer dendritic cells also dependent on ASMase? What is the mechanism of release of the cytolytic effector molecules from the matrix? Is ASMase also critical for the secretion of IFN-γ by $CD4^+$ helper T cells or natural killer cells and does it affect the release of other cytokines that follow the synaptic secretory pathway (such as interleukins 2 and 10) or multidirectional secretory pathway (such as TNF, CCL3 (MIP-1α), CCL4 (MIP-2β) and interleukin 4)? The answer to these questions will show whether ASMase functions as a 'tailor' with a broader repertoire in the immune system.

1. Henkart, P.A. & Catalfamo, M. *Adv. Immunol.* **83**, 233–252 (2004).
2. Herz, J. *et al. Nat. Immunol.* **10**, 761–768 (2009).
3. Raja, S.M. *et al. J. Biol. Chem.* **277**, 49523–49530 (2002).
4. Stinchcombe, J.C. & Griffiths, G.M. *Annu. Rev. Cell Dev. Biol.* **23**, 495–517 (2007).
5. Smith, E.L. & Schuchman, E.H. *FASEB J.* **22**, 3419–3431 (2008).
6. Utermöhlen, O., Karow, U., Lohler, J. & Krönke, M. *J. Immunol.* **170**, 2621–2628 (2003).
7. Schramm, M., Herz, J., Haas, A., Krönke, M. & Utermöhlen, O. *Cell. Microbiol.* **10**, 1839–1853 (2008).
8. Makedonas, G. *et al. J. Immunol.* **182**, 5560–5569 (2009).
9. Kelly, R.B. *Science* **230**, 25–32 (1985).
10. Poo, W.J., Conrad, L. & Janeway, C.A. Jr. *Nature* **332**, 378–380 (1988).
11. Huse, M., Quann, E.J. & Davis, M.M. *Nat. Immunol.* **9**, 1105–1111 (2008).
12. Catalfamo, M. *et al. Immunity* **20**, 219–230 (2004).

A novel modifier of regulatory T cells

Naganari Ohkura & Shimon Sakaguchi

The receptor for the lipid mediator sphingosine 1-phosphate is critical for T cell trafficking. New data show that signaling mediated by this receptor critically controls the development, maintenance and suppressive activity of natural regulatory T cells that express the transcription factor Foxp3.

Naturally occurring regulatory T cells (T_{reg} cells) that express the transcription factor Foxp3 are indispensable for the maintenance of immunological self-tolerance and immune homeostasis[1]. The balance between T_{reg} cells and effector T cells is critical for the inhibition of autoimmune disease and for proper control of the quality and magnitude of adaptive immune responses. A variety of molecules influence this balance by affecting the generation, survival, trafficking and function of the two populations in different ways. In this issue of *Nature Immunology*, Liu *et al.* demonstrate that the receptor for sphingosine 1-phosphate (S1P), a lipid mediator abundant in the serum, is one such molecule[2]. S1P receptor type 1 ($S1P_1$) delivers an intrinsic negative signal to $Foxp3^+$ T_{reg} cells in controlling their thymic generation, peripheral maintenance and suppressive activity. Liu *et al.* also show that the signal through $S1P_1$ specifically activates the Akt-mTOR kinase pathway in T_{reg} cells and thereby controls their function.

S1P signals through the G protein–coupled receptors $S1P_1$–$S1P_5$. Studies have identified an important function of $S1P_1$ in promoting the egress of T cells from the lymphoid organs[3]. Liu *et al.* address the possible contribution of $S1P_1$ to the function of $Foxp3^+$ natural T_{reg} cells with an elegant set of loss- and gain-of-function genetic approaches[2]. They first create a mouse line with T cell–specific deficiency of $S1P_1$ and find that these mice have more T cells that express Foxp3 and the immunomodulatory receptors CTLA-4 and GITR, all characteristics of T_{reg} cells. Notably, $S1P_1$-knockout T_{reg} cells have a much greater capacity than do wild-type T_{reg} cells to suppress the *in vitro* proliferation and production of interleukin 2 (IL-2) of conventional T cells (T_{conv} cells), whereas these T_{reg} cells have a defect in their egress from thymus. The authors also create $S1P_1$-transgenic mice in which T cells have high expression of $S1P_1$ driven by the human *CD2* promoter-enhancer. The mice have considerably fewer $Foxp3^+$ CD4 single-positive cells in the thymus, and their $S1P_1$-overexpressing T_{reg} cells are much less efficient in suppressing T_{conv} cells. Notably, in a model of colitis induced by the transfer of T_{conv} cells into lymphopenic mice, cotransfer of T_{reg} cells from $S1P_1$-transgenic mice fails to prevent colitis, whereas cotransfer of T_{reg} cells from wild-type mice does prevent colitis. Thus, the enhanced signaling through $S1P_1$ induces spontaneous autoimmunity due to dysfunction of T_{reg} cells. These two lines of evidence obtained by $S1P_1$ deficiency and overexpression collectively suggest that $S1P_1$ signaling negatively regulates both the thymic generation and suppressive activity of T_{reg} cells (Fig. 1). Thus, the $S1P_1$ pathway has a unique function in natural T_{reg} cells, as it couples the trafficking and intrinsic function of T_{reg} cells.

Pursuing the mechanism by which $S1P_1$ signaling leads to diminished function of T_{reg} cells, Liu *et al.* observe that LY294002, an inhibitor

Naganari Ohkura and Shimon Sakaguchi are in the Department of Experimental Pathology, Institute for Frontier Medical Sciences, Kyoto University, Kyoto, Japan, and World Premier International Research Center, Immunology Frontier Research Center, Osaka University, Suita, Japan.
e-mail: shimon@frontier.kyoto-u.ac.jp

of phosphatidylinositol-3-OH kinase (PI(3)K), and the mTOR inhibitor rapamycin are able to restore the differentiation of $S1P_1$-transgenic T cells into T_{reg} cells, which indicates specific involvement of the mTOR pathway in $S1P_1$ signaling[2]. These findings are consistent with the idea that the PI(3)K-Akt-mTOR pathway is involved in the differentiation and function of T_{reg} cells. For example, the thymi of PI(3)K-deficient mice have more T_{reg} cells[4]; constitutively active Akt diminishes transforming growth factor-β–induced transcription of *Foxp3* (ref. 5); and inhibition of mTOR promotes T_{reg} cell differentiation[6]. Such findings collectively suggest that the $S1P_1$-PI(3)K-Akt-mTOR pathway is critical for the differentiation and function of T_{reg} cells.

How, then, does $S1P_1$ control the trafficking and function of natural T_{reg} cells? Although the authors demonstrate the importance of $S1P_1$ for the development and function of natural T_{reg} cells, the role of its ligands in T_{reg} cell function is obscure. The endogenous ligand of $S1P_1$, S1P, is a circulating bioactive lipid metabolite that has been known for many years to have various biological effects, including platelet aggregation, insulin- and growth factor–induced responses, and the growth and differentiation of many cell types. S1P is contained in platelets and erythrocytes at high concentrations and is bound to albumin and high-density lipoprotein in the circulation. The involvement of lipid-mediated signaling in T_{reg} cell function will be an important area of future research. Another point is the relevance of the relative expression of $S1P_1$ to the function of lymphocytes. $S1P_1$ mRNA can be detected in various cells of the immune system, including T_{reg} cells and T_{conv} cells. Liu *et al.* show that after stimulation with Il-2 and antibody to the T cell antigen receptor, $S1P_1$ mRNA decreases abruptly in T_{conv} cells, whereas it is gradually downregulated in T_{reg} cells[2]. Therefore, they propose a model that differences in the expression of $S1P_1$ at early and late stages of immune activation affect both the egress of lymphocytes and T_{reg} cell activity. It remains to be determined how the expression of $S1P_1$ and its degradation are properly controlled in T_{reg} cells and T_{conv} cells.

Despite those uncertainties, this study provides strong evidence of an unexpected immunoregulatory function for $S1P_1$ in T_{reg} cells. Abundant expression of $S1P_1$ is directly associated with enhancement of immune responses, whereas low expression of this molecule is associated with immune suppression through the Akt-mTOR pathway in T_{reg} cells. Therefore, $S1P_1$ would be a potential target for the treatment of immunological diseases and for the control of physiological immune responses. In fact, FTY720, a structural analog of sphingosine, has been shown to control some autoimmune and allergic diseases and to suppress the rejection of transplanted organs[7]. This drug is now in phase III clinical trials for the treatment of multiple sclerosis. However, the biochemical basis of the effect of FTY720 is not completely understood. FTY720 is thought to be an antagonist of $S1P_1$, but after being phosphorylated, it mimics the action of S1P and acts as an agonist for four of the five S1P receptors[8]. Moreover, it has been reported that the effect of FTY720 on mast cells is independent of its phosphorylation and S1P receptor functions[9]. Given that the effects of $S1P_1$ deficiency are similar to those of FTY720, it is likely that the drug acts as an antagonist to inactivate $S1P_1$ in T_{reg} cells. Understanding of molecular details of $S1P_1$ signaling is critical for the optimal manipulation of immune responses by FTY720.

One important issue of T_{reg} cell research at present is understanding how T_{reg} cell lineage and activity are controlled in response to extracellular stimuli. Liu *et al.* show that $S1P_1$ serves as a unique receptor system that negatively regulates the function of T_{reg} cells[2]. However, various stimuli positively control T_{reg} function through accessory molecules. For example, CD28 is required for T_{reg} cell development in the thymus[10]. Costimulation through GITR or OX40 facilitates T_{reg} proliferation in the presence of IL-2 (ref. 11). T_{reg} populations can also expand after stimulation through Toll-like receptors[12]. Such findings collectively suggest that T_{reg} cells are regulated positively and negatively by the coordination of dozens of signaling pathways, including the $S1P_1$-PI(3)K-Akt-mTOR pathway. How such positive and negative signals are integrated to exert a particular T_{reg} function is a key issue for future research aiming to control T_{reg} cells for the benefit of the host (Fig. 1).

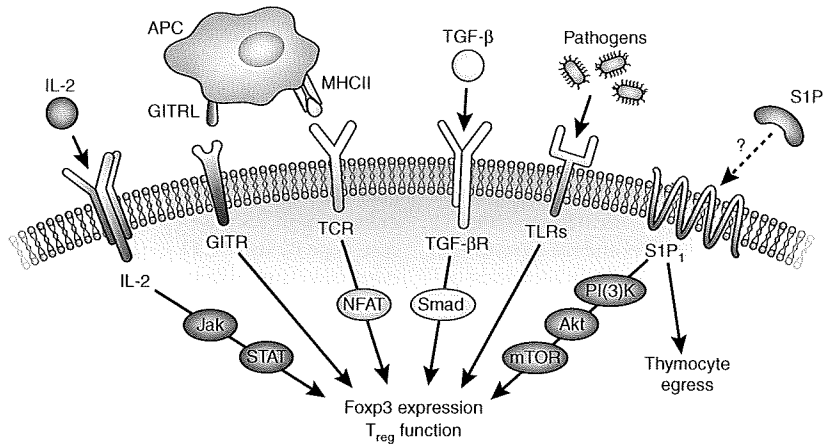

Figure 1 T_{reg} cell function is controlled by many signaling pathways, including the $S1P_1$-mediated pathway. T_{reg} cells constitutively express dozens of receptors, such as IL-2R (CD25), GITR, T cell antigen receptor (TCR), the receptor for transforming growth factor-β (TGF-βR), Toll-like receptors (TLRs) and receptors for S1P. $S1P_1$ delivers negative signal for the thymic generation, peripheral maintenance and suppressive activity of T_{reg} cells through the $S1P_1$-PI(3)K-Akt-mTOR signaling pathway. APC, antigen-presenting cell; GITRL, GITR ligand; MHCII, major histocompatibility complex II; Jak, Janus kinase; STAT, signal transducer and activator of transcription; NFAT, nuclear factor of activated T cells; Smad, signal transducer of bone-morphogenetic protein.

In conclusion, the study by Liu *et al.* in this issue of *Nature Immunology* has identified previously unknown functions of $S1P_1$ in supporting the development, maintenance and function of $Foxp3^+$ natural T_{reg} cells. It opens new avenues for the investigation of lipid-mediated immune regulation. Moreover, elucidating the $S1P_1$-PI(3)K-Akt-mTOR pathway will provide important clues for the development of new therapeutic agents for controlling physiological and pathological immune responses.

1. Sakaguchi, S. *et al. Cell* **133**, 775–787 (2008).
2. Liu, G. *et al. Nat. Immunol.* **10**, 769–777 (2009).
3. Matloubian, M. *et al. Nature* **427**, 355–360 (2004).
4. Patton, D.T. *et al. J. Immunol.* **177**, 6598–6602 (2006).
5. Haxhinasto, S., Mathis, D. & Benoist, C. *J. Exp. Med.* **205**, 565–574 (2008).
6. Gao, W. *et al. Am. J. Transplant.* **7**, 1722–1732 (2007).
7. Zhang, Z. & Schluesener, H.J. *Mini Rev. Med. Chem.* **7**, 845–850 (2007).
8. Brinkmann, V. *et al. J. Biol. Chem.* **277**, 21453–21457 (2002).
9. Payne, S.G. *et al. Blood* **109**, 1077–1085 (2007).
10. Golovina, T.N. *et al. J. Immunol.* **181**, 2855–2868 (2008).
11. McHugh, R.S. *et al. Immunity* **16**, 311–323 (2002).
12. Sutmuller, R.P. *et al. Trends Immunol.* **27**, 387–393 (2006).

Immunity
Resource

Functional Delineation and Differentiation Dynamics of Human CD4$^+$ T Cells Expressing the FoxP3 Transcription Factor

Makoto Miyara,[1,10] Yumiko Yoshioka,[1,9] Akihiko Kitoh,[1,9] Tomoko Shima,[1,9] Kajsa Wing,[1] Akira Niwa,[2] Christophe Parizot,[3] Cécile Taflin,[3] Toshio Heike,[2] Dominique Valeyre,[4] Alexis Mathian,[3] Tatsutoshi Nakahata,[2] Tomoyuki Yamaguchi,[1] Takashi Nomura,[1] Masahiro Ono,[1] Zahir Amoura,[5,6] Guy Gorochov,[3,6] and Shimon Sakaguchi[1,7,8,*]

[1]Department of Experimental Pathology, Institute for Frontier Medical Sciences
[2]Department of Pediatrics, Graduate School of Medicine
Kyoto University, Kyoto 606-8507, Japan
[3]Institut National de la Santé et de la Recherche Médicale (INSERM) UMR-S 945, Laboratoire AP-HP d'immunologie cellulaire et tissulaire, Hôpital Pitié-Salpêtrière, 75013 Paris, France
[4]Pneumology Department, AP-HP Hôpital Avicenne, 93000 Bobigny, France
[5]Internal Medicine Department, AP-HP Hôpital Pitié-Salpêtrière, 75013 Paris, France
[6]Pierre and Marie Curie University, UPMC Paris Universitas, 75005 Paris, France
[7]Core Research for Evolutional Science and Technology (CREST), Japan Science and Technology Agency, Kawaguchi 332-0012, Japan
[8]WPI Immunology Frontier Research Center, Osaka University, Suita 565-0871, Japan
[9]These authors contributed equally to this work
[10]Present address: Internal Medicine Department and Institut National de la Santé et de la Recherche Médicale (INSERM) UMR-S 945, Laboratoire AP-HP d'immunologie cellulaire et tissulaire, Hôpital Pitié-Salpêtrière, 75013 Paris, France
*Correspondence: shimon@frontier.kyoto-u.ac.jp
DOI 10.1016/j.immuni.2009.03.019

SUMMARY

FoxP3 is a key transcription factor for the development and function of natural CD4$^+$ regulatory T cells (Treg cells). Here we show that human FoxP3$^+$CD4$^+$ T cells were composed of three phenotypically and functionally distinct subpopulations: CD45RA$^+$FoxP3^{lo} resting Treg cells (rTreg cells) and CD45RA$^-$FoxP3^{hi} activated Treg cells (aTreg cells), both of which were suppressive in vitro, and cytokine-secreting CD45RA$^-$FoxP3^{lo} nonsuppressive T cells. The proportion of the three subpopulations differed between cord blood, aged individuals, and patients with immunological diseases. Terminally differentiated aTreg cells rapidly died whereas rTreg cells proliferated and converted into aTreg cells in vitro and in vivo. This was shown by the transfer of rTreg cells into NOD-scid-common γ-chain-deficient mice and by TCR sequence-based T cell clonotype tracing in peripheral blood in a normal individual. Taken together, the dissection of FoxP3$^+$ cells into subsets enables one to analyze Treg cell differentiation dynamics and interactions in normal and disease states, and to control immune responses through manipulating particular FoxP3$^+$ subpopulations.

INTRODUCTION

FoxP3-expressing CD4$^+$ thymus-derived naturally occurring regulatory T cells (Treg cells) play an indispensable role for the maintenance of self tolerance and immune homeostasis (Sakaguchi et al., 2008). They play crucial roles in human diseases, such as autoimmune disease, allergy, and cancer (Curiel et al., 2004; Ehrenstein et al., 2004; Kriegel et al., 2004; Miyara et al., 2005; Viglietta et al., 2004). Human natural Treg cells were initially defined according to their high expression of CD25 (Baecher-Allan et al., 2001; Dieckmann et al., 2001; Jonuleit et al., 2001; Levings et al., 2001; Ng et al., 2001; Taams et al., 2001), based on the finding that murine CD25$^+$CD4$^+$ T cells are highly suppressive (Sakaguchi et al., 1995). With the discovery of FoxP3 as a "master control gene" for CD4$^+$ Treg cell development and function (Fontenot et al., 2003; Hori et al., 2003; Khattri et al., 2003), detection of FoxP3 at the mRNA and protein level revealed that human CD25^{hi}CD4$^+$ T cells indeed express FoxP3 (Miyara et al., 2006; Roncador et al., 2005; Yagi et al., 2004). In contrast to murine FoxP3$^+$ Treg cells, however, human FoxP3$^+$ cells may not be functionally homogenous. For example, it has been reported that mere TCR stimulation can induce FoxP3 expression in apparently naive human FoxP3$^-$CD4$^+$ T cells without conferring suppressive activity (Allan et al., 2007; Gavin et al., 2006; Tran et al., 2007; Wang et al., 2007). Furthermore, some FoxP3$^+$ cells are phenotypically naive (e.g., CD45RA$^+$), present in cord blood as well as in peripheral blood of adults, and suppressive in vitro (Valmori et al., 2005), whereas other FoxP3$^+$ cells phenotypically resemble memory T cells (e.g., CD45RA$^-$) and are suggested to originate from peripheral memory FoxP3$^-$CD4$^+$ T cells (Vukmanovic-Stejic et al., 2006). To better understand the roles of FoxP3$^+$ T cells for the control of immune responses, it is necessary to determine whether FoxP3-expressing T cells in freshly isolated CD4$^+$ T cells are functionally heterogeneous, how functionally different subpopulations of FoxP3$^+$ cells can be reliably delineated, and how such

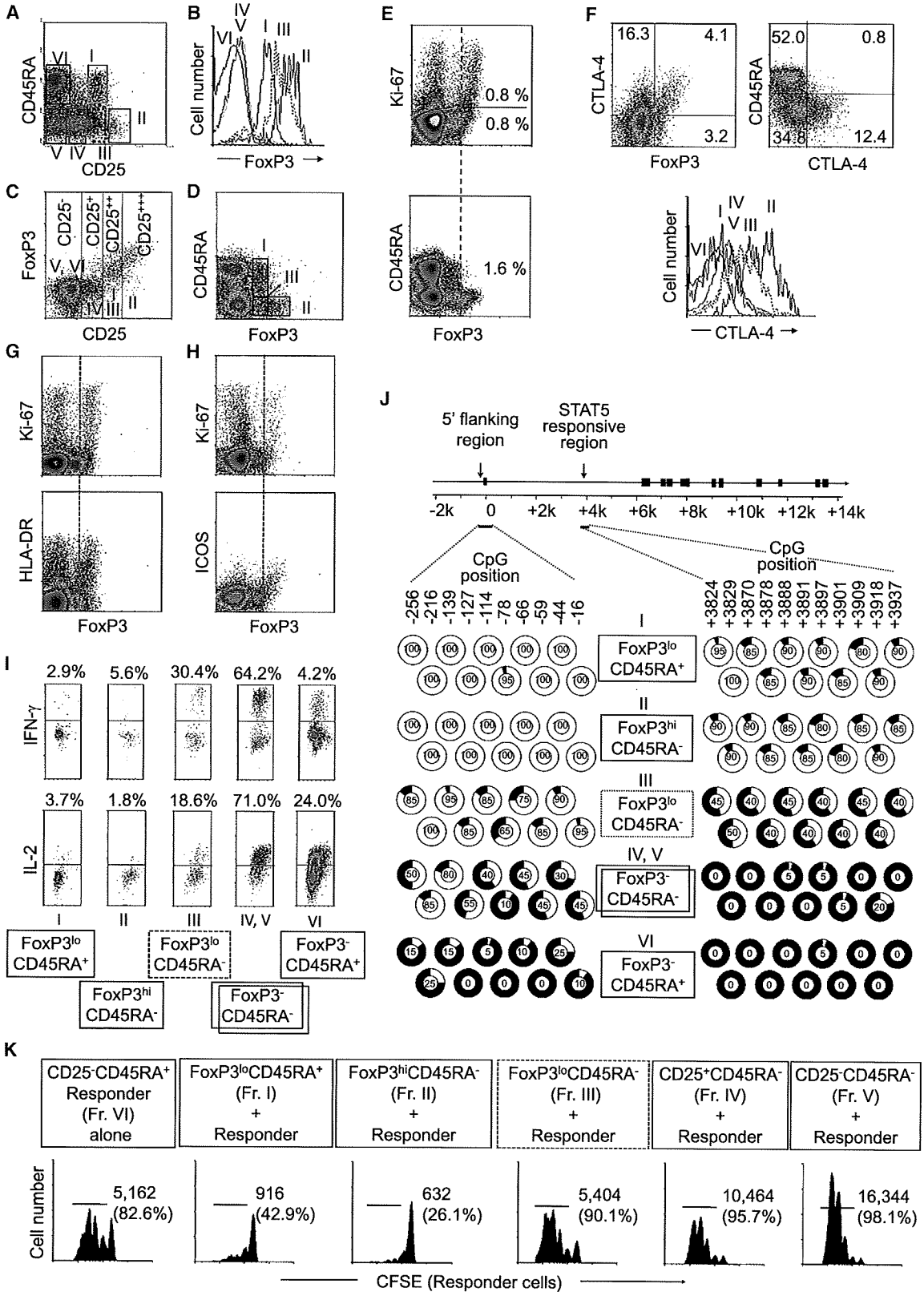
A
CD45RA
CD25
B
Cell number
FoxP3
C
FoxP3
CD25
D
CD45RA
FoxP3
E
Ki-67
0.8 %
0.8 %
CD45RA
1.6 %
FoxP3
F
CTLA-4
16.3
4.1
3.2
FoxP3
CD45RA
52.0
0.8
34.8
12.4
CTLA-4
Cell number
CTLA-4
G
Ki-67
HLA-DR
FoxP3
H
Ki-67
ICOS
FoxP3
I
IFN-γ
IL-2
2.9%
5.6%
30.4%
64.2%
4.2%
3.7%
1.8%
18.6%
71.0%
24.0%
FoxP3lo CD45RA+
FoxP3hi CD45RA-
FoxP3lo CD45RA-
FoxP3- CD45RA-
FoxP3- CD45RA+
J
5' flanking region
STAT5 responsive region
-2k
0
+2k
+4k
+6k
+8k
+10k
+12k
+14k
CpG position
CpG position
FoxP3lo CD45RA+
FoxP3hi CD45RA-
FoxP3lo CD45RA-
FoxP3- CD45RA-
FoxP3- CD45RA+
K
CD25-CD45RA+ Responder (Fr. VI) alone
FoxP3loCD45RA+ (Fr. I) + Responder
FoxP3hiCD45RA- (Fr. II) + Responder
FoxP3loCD45RA- (Fr. III) + Responder
CD25+CD45RA- (Fr. IV) + Responder
CD25-CD45RA- (Fr. V) + Responder
Cell number
5,162 (82.6%)
916 (42.9%)
632 (26.1%)
5,404 (90.1%)
10,464 (95.7%)
16,344 (98.1%)
CFSE (Responder cells)

subsets differentiate and interact in physiological and disease states.

In this report, we show that human FoxP3$^+$CD4$^+$ T cells can be separated into three functionally and phenotypically different subpopulations based on the expression of FoxP3, cell surface phenotype, the degree of DNA methylation of the FoxP3 gene, DNA microarray profile, proliferation status in the physiological state, cytokine secreting capacity, TCR repertoire, and in vitro suppressive activity. These populations are (1) CD45RA$^+$FoxP3^{lo} resting Treg cells, (2) CD45RA$^-$FoxP3^{hi} activated Treg cells, and (3) cytokine-secreting CD45RA$^-$FoxP3^{lo} non-Treg cells. With this dissection of FoxP3$^+$ T cells into subpopulations, we show the dynamics of Treg cell differentiation in vitro, in vivo, and ex vivo in normal and disease states. The results indicate that functional and numerical analysis of each FoxP3$^+$ subset is essential for assessing immunological states, and that manipulation of a particular subset, rather than whole FoxP3$^+$ cells, helps to dampen or augment a variety of physiological and pathological immune responses.

RESULTS

Separation of FoxP3$^+$CD4$^+$ T Cells into Three Subpopulations by the Expression of FoxP3, CD25, and CD45RA

The combination of CD25 and CD45RA staining of CD4$^+$ T cells in peripheral blood lymphocytes (PBL) of normal healthy individuals revealed six subpopulations (Fraction [Fr.] I–VI) that expressed the FoxP3 protein at different amounts (Figures 1A and 1B). Among them, Fr. I, II, and III were FoxP3$^+$ (Figure 1B) and the degree of FoxP3 expression in these fractions were proportional to CD25 expression (Figure 1C). Notably, these three FoxP3$^+$ populations could be distinctly separated by the combination of FoxP3 and CD45RA staining; i.e., FoxP3^{lo}CD45RA$^+$ cells, which were CD25^{++} (Fr. I), FoxP3^{hi}CD45RA$^-$ cells, which were CD25^{+++} (Fr. II), and FoxP3^{lo}CD45RA$^-$ cells, which were CD25^{++} (Fr. III) (Figure 1D). The fractions could be prepared as live cells by cell sorting as CD25^{++}CD45RA$^+$, CD25^{+++}CD45RA$^-$, and CD25^{++}CD45RA$^-$ cells, respectively (Figure S1A available online). Purified Fr. I, II, and III populations expressed FoxP3 transcripts to a similar degree irrespective of different amounts of FoxP3 protein expressed in each population (Figure 1B; Figure S1B). Fr. IV formed a distinct population as CD25$^+$FoxP3$^-$ cells (Figure 1C), but it was not well demarcated from Fr. V by CD45RA or CD25 staining (Figure 1A). Therefore, we analyzed Fr. IV and V together in the functional examination of FoxP3$^+$ subsets (see below).

Assessment of the proliferative status of each subpopulation in the physiological state by detecting the expression of Ki-67, a nuclear protein expressed in cells ready to proliferate and at a higher amount in actually proliferating cells (Figure S2), revealed that about half of the cells in Fr. II were proliferating whereas the cells in Fr. I and III were not (red dotted line in Figure 1E). Fr. II expressed intracellular CTLA-4 to the highest degree whereas Fr. I hardly expressed the molecule (Figure 1F). Furthermore, Fr. II corresponded to HLA-DR-expressing and also ICOS-expressing FoxP3$^+$ cells as reported by others (Figures 1G and 1H; Baecher-Allan et al., 2006; Ito et al., 2008).

Analysis of cytokine production by each fraction showed that Fr. II scarcely produced IL-2 or IFN-γ. Among FoxP3^{lo} cells, Fr. I was poor producer of IL-2 and IFN-γ whereas Fr. III produced high amounts of these cytokines (Figure 1I; Figure S3).

The 5′ flanking region and a STAT5-responsive region in the intron 1 of the *FOXP3* gene are critical for induction and enhancement of FoxP3 expression by TCR and IL-2 stimulation (Floess et al., 2007; Mantel et al., 2006; Zorn et al., 2006). Analysis of the DNA methylation status of these regions in each fraction prepared from a male donor showed that the CpG methylation sites in the regions were completely demethylated in Fr. I and Fr. II (Figure 1J). The 5′ flanking region of Fr. III was also highly demethylated, although the demethylation pattern was less uniform compared with Fr. I and II. In contrast, their STAT5-responsive region was less demethylated than other FoxP3$^+$ subsets. In addition, memory-like CD25$^+$ and CD25$^-$ CD45RA$^-$CD4$^+$ non-Treg cells (Fr. IV, V), which were FoxP3$^-$, had their 5′ flanking region moderately demethylated whereas the STAT5 responsive region was virtually completely methylated. Both regions were highly methylated in naive Fr. VI. These findings were confirmed by analysis of individual clones isolated from each subpopulation (Figure S4). The results collectively

Figure 1. Delineation of FoxP3$^+$CD4$^+$ T Cells into Subsets by Cell Surface Molecules, Proliferative State, Cytokine Production, Methylation Status of the *FOXP3* Gene, and In Vitro Suppressive Activity

(A–D) Six subsets of CD4$^+$ T cells defined by the expression of CD45RA and CD25: pink line (Fraction [Fr.] I), CD25^{++}CD45RA$^+$ cells; bold red line (Fr. II), CD25^{+++}CD45RA$^-$ cells; broken brown line (Fr. III), CD25^{++}CD45RA$^-$ cells; green line (Fr. IV), CD25$^+$CD45RA$^-$ cells; blue line (Fr. V), CD25$^-$CD45RA$^-$ cells; black line (Fr. VI), CD25$^-$CD45RA$^+$ cells. Expression of FoxP3 (B), CD25 and intracellular FoxP3 (C), and CD45RA and FoxP3 (D) in each fraction shown in (A). Data are representative of 19 blood donors.

(E) Flow cytometry of the expression of nuclear Ki-67 and FoxP3 in CD4$^+$ T cells. Red broken line separates Ki-67$^+$FoxP3^{hi} from Ki-67$^-$FoxP3^{lo} cells and CD45RA$^+$FoxP3^{lo} from CD45RA$^-$FoxP3^{hi} cells. The percentages of Ki-67$^+$ and Ki-67$^-$FoxP3^{hi} cells among CD4$^+$ cells are indicated in the top panel and the percentage of FoxP3^{hi}CD45RA$^-$ cells in the bottom panel.

(F) Flow cytometry of the expression of intracellular CTLA-4 and FoxP3 (top left); CD45RA and CTLA-4 (top right) by CD4$^+$ T cells; and expression of CTLA-4 by each fraction defined in (A)–(D) (bottom). Numbers indicate percent of cells in each quadrant.

(G and H) Expression of Ki-67 and FoxP3 (top) and of HLA-DR or ICOS and FoxP3 (bottom). Red broken line separates Ki-67$^+$FoxP3^{hi} from Ki-67$^-$FoxP3^{lo} cells and HLA-DR$^-$FoxP3^{lo} from HLA-DR$^+$FoxP3^{hi} cells (G) or ICOS$^-$FoxP3^{lo} from ICOS$^+$FoxP3^{hi} cells (H).

(I) Production of IFN-γ, IL-2 by each fraction after stimulation with PMA + ionomycin, and percent of cytokine-secreting cells in each fraction is shown. Data are representative of six independent experiments.

(J) Analysis of DNA methylation status at 5′ flanking region (left) and STAT5-responsive (right) region of the *FOXP3* gene in FoxP3-expressing or -nonexpressing CD4$^+$ T cell subsets (Figure S1) from PBMCs of one healthy male donor. Percentages of clones displaying demethylation of indicated CpG methylation sites are indicated and depicted in white in sector graphs. 19 to 20 clones were sequenced from each CD4$^+$ T cell subset.

(K) CFSE dilution by 10^4 labeled CD25$^-$CD45RA$^+$CD4$^+$ responder T cells assessed after 84–90 hr of TCR-stimulated coculture with indicated CD4$^+$ T cell subset at a 1 to 1 ratio. Cell number and percentage of dividing cells per well are indicated. Data are representative of 12 separate experiments.

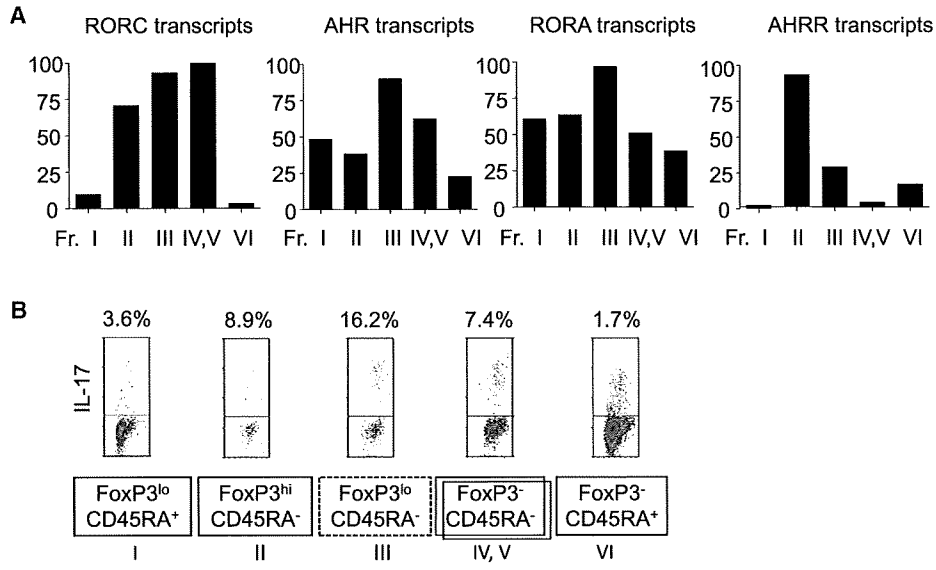

Figure 2. CD45RA$^-$ FoxP3^{lo}CD4$^+$ T Cells Contain Cells with Th17 Cell Potential

(A) The amounts of transcripts of indicated genes in separated CD4$^+$ T cell subsets were assessed by quantitative PCR.

(B) Flow cytometry of the production of IL-17 by gated CD4$^+$ T cell subsets after stimulation with PMA + ionomycin for 5 hr. Percentages of cytokine-secreting cells are shown. Data are representative of six independent experiments.

indicate that Fr. I and II are active in FoxP3 gene transcription and close in their differentiation stage, and that, compared with these fractions, Fr. III may be less capable of maintaining FoxP3 expression in the presence of IL-2 and STAT5 signaling.

To assess the in vitro suppressive potency of each fraction, we measured the extent of CFSE dilution of labeled naive CD25$^-$CD45RA$^+$CD4$^+$ T cells (hereafter called responder cells) cocultured with an equal number of each fraction and stimulated for 4 days (Figure 1K). Fr. I and II (isolated as CD25^{++}CD45RA$^+$ and CD25^{+++}CD45RA$^-$ cells, respectively, as shown in Figure S1) potently suppressed the proliferation of responder cells, whereas Fr. III, IV, and V did not and even enhanced the responder proliferation. The inability of Fr. III (CD45RA$^-$Foxp3^{lo} cells) to suppress was confirmed by using CD127 as an additional marker for purifying FoxP3-expressing cells from CD4$^+$ T cells (Figure S5; Liu et al., 2006; Seddiki et al., 2006).

Taken together, three distinct subpopulations of FoxP3$^+$CD4$^+$ T cells can be defined in human PBL by the expression of CD45RA and FoxP3 as summarized in Table S1; i.e., Fr. I: CTLA-4^{lo}Ki-67$^-$CD45RA$^+$FoxP3^{lo} T cells; Fr. II: CTLA-4^{hi}CD45RA$^-$FoxP3^{hi} cells, both of which possess a fully functional *FOXP3* gene, hardly secrete cytokines, and potently suppress proliferation; and Fr. III: CTLA-4^{int}CD45RA$^-$FoxP3^{lo} T cells, which secrete cytokines, are much less active in the expression of the *FOXP3* gene under the control via STAT5, and do not suppress proliferation in vitro. Based on their phenotypic and functional characteristics, Fr. I and Fr. II can be designated as resting Treg cells (rTreg cells) and activated Treg cells (aTreg cells), respectively.

FoxP3^{lo}CD45RA$^-$ Nonregulatory T Cells Contain Cells with Th17 Cell Potential

DNA microarray analysis of each fraction showed that the gene expression patterns in the three FoxP3-expressing subpopulations were distinct (Figure S6A). Quantitative assessment of mRNA expression of differentially expressed genes revealed that the expression of RORC, a key transcription factor in Th17 cell lineage (Ivanov et al., 2006), was highly upregulated in Fr. II and III, indicating that RORC-FoxP3 double-positive population, which was recently described in mice (Yang et al., 2008a; Zhou et al., 2008), exists in humans as well in Fr. II and III (Figure S6B). Transcripts encoding RORα and AHR, both of which contribute to Th17 cell differentiation in mice (Veldhoen et al., 2008; Yang et al., 2008b), were highly upregulated in Fr.III, further indicating that this population contains cells with Th17 cell potential (Figure 2A). Also of note is that Fr. II specifically expressed high amounts of AHR repressor transcripts, suggesting that Treg cell differentiation might accompany an inhibition of Th17 cell differentiation via expression of AHR repressor. Assessment of cytokine production revealed that Fr. III was the highest producer of IL-17 even compared with naive FoxP3$^-$CD45RA$^+$ (Fr. VI) or memory-like FoxP3$^-$CD45RA$^-$CD4$^+$ non-Treg cells (Fr. IV and V) (Figure 2B; Figure S3).

Thus, DNA microarray profiling of FoxP3$^+$ subpopulations supports the relevance of separating FoxP3$^+$CD4$^+$ T cells into three subsets. Further, regarding the cell lineage relationship of FoxP3$^+$ cells and Th17 cells, Fr. III contains FoxP3-RORγ double-positive cells with a Th17 cell potential, in addition to IL-2- and/or IFN-γ-producing cells (Figure 1I).

Resting Treg Cells Proliferate whereas Activated Treg Cells Die while Suppressing In Vitro

As shown in Figure 1E, fresh Fr. I cells (rTreg cells) did not express Ki-67. However, when they were cocultured with responder cells and TCR stimulated, all the FoxP3-expressing cells became Ki-67$^+$ on day 4, indicating that rTreg cells proliferate (Figure S7). Assessment of proliferation by CFSE dilution during 4 days of culture also revealed that both aTreg cells